



The Effects of Size and Shape  
Changes on Motility in *Escherichia*  
*coli* (AW405)

Being a Thesis Submitted in Fulfilment of the Requirements for  
the Degree of Masters of Biology (M.Sc.)  
at the University of Hull.

Katie Louise Thornton B.Sc. (Hons)

**(September 2015)**



# Contents

<b>Figures</b> .....	4
<b>Abstract</b> .....	7
<b>Acknowledgments</b> .....	8
<b>Chapter 1:</b> .....	9
<b>1.0. Introduction</b> .....	10
1.1. Size in Nature – From the Macroscopic to the Microscopic World.....	10
1.2. The Relationship Between Size and Motility in Bacteria .....	15
1.3. Motile Cell Shape .....	18
1.4. Mechanisms for Motility .....	19
1.5. The Random Walk Model .....	22
1.6. Ballistic and Diffusive Movement .....	23
1.7. Study Species .....	24
1.7.1. Bacterial Strain .....	24
1.7.2. Cell Culture.....	25
1.8. <i>Escherichia coli</i> Movement.....	25
1.9. Project Aims .....	28
<b>Chapter 2:</b> .....	29
<b>2.0. The Effect of Changes in Cell Aspect Ratio on Locomotory Behaviours ...</b>	<b>30</b>
2.1. Introduction .....	30
2.1.1. Antibiotic Treatments .....	31

2.1.2 Filamentous Cells of <i>Escherichia coli</i> .....	33
2.2 Methods .....	35
2.2.1. Cell Preparation .....	35
2.2.2. Cephalixin Treatment.....	35
2.2.3. Slide Selection .....	36
2.2.4. Video Acquisition .....	37
2.2.5. Video Analysis.....	38
2.2.6. Runs and Tumbles .....	41
2.3. Data Analysis .....	42
2.4. Results.....	43
2.5. Discussion of Results .....	50
2.6. Conclusions .....	53
<b>Chapter 3:</b> .....	<b>55</b>
<b>3.0 General Discussion</b> .....	<b>56</b>
3.1.1 3D Tracking.....	56
3.1.2 Wall Effects .....	57
3.2. Outstanding Questions .....	58
3.2.1. What Effect does Filamentation Have on Chemotactic Responses? .....	58
3.2.2. How do Changes in Cell Shape Affect Motility? The Study of Spherical <i>E. coli</i> and other Shapes compared with Filamentous and Untreated Forms.....	60
<b>References</b> .....	<b>63</b>

## Figures

**Figure 1:** Comparison of Reynolds numbers for different organisms with increasing size, highlighting the dominant forces present at each scale (From Nachtigall, 1981).13

**Figure 2:** Body length plotted against swimming speed as a measure of body lengths per second for a variety of micro-organisms. Circular markers denote the flagellated species, the triangular markers denote the ciliates, and the diamond marker denotes the bacterial species *Vibrio harvevi* (Vogel, 2008)..... 17

**Figure 3:** Examples of the diverse array of prokaryotic shapes currently recorded (From Young, 2006). All cells are drawn to scale, colours are for emphasis only.....**Error!**

**Bookmark not defined.**

**Figure 4:** Structure of a single bacterial flagellum. Figure highlights the position of each of the Flg and Fli proteins, and the general structure of the organelle (From Berg, 2003). ..... 21

**Figure 5:** Model swimming cell; arrows denote the direction of fluid flow generated by a singular rotating flagellum (From Sleight, 1991)..... 21

**Figure 6:** A typical track following the random movement of 'runs' and 'tumbles' of a single *E. coli* cell, produced using a custom-built tracking microscope (From Berg & Brown, 1972). ..... 27

**Figure 7:** An example of *E. coli* flagella movements during one complete run-tumble cycle (From Darnton et al., 2006). By the end of the tumbling period (stage 4), the reversed flagellum has become tightly curled and the cell has re-orientated into a new directionality of movement. .... 27

**Figure 8:** Cell wall structure of rod-shaped prokaryotes. The purple patches forming a helical pattern are the actin-like filaments (MreB) which give the cell its rod structure. The blue and green patches in the centre of the cell are the FtsZ and FtsA filaments involved in cell division (Juarez & Margolin, 2012). ..... 31

<b>Figure 9:</b> The various stages of natural prokaryotic cell division, highlighting the role of the FtsZ protein (Z-Ring) in the division process (Margolin, 2005). .....	32
<b>Figure 10:</b> Phase contrast microscope image (x1000 magnification) of filamentous E. coli cells. Cells treated with cephalixin and incubated for 24 hours to produce maximum lengths of up to 50 micrometres in length. ....	34
<b>Figure 11:</b> Matlab thresholding process, used to isolate cells for tracking and create a measure of cell shape properties. ....	39
<b>Figure 12:</b> Cell size and shape statistics for each cell isolated within one two-minute video. Frequency histograms of longest axial length ( $\mu\text{m}$ ) (top left), width – perpendicular to axial length ( $\mu\text{m}$ ) (top right), aspect ratio (bottom left) and volume (bottom right) ( $\mu\text{m}^3$ ).....	40
<b>Figure 13:</b> Visualization of all tracks recorded for an example two minute video (distance is in micrometres). (Colours are used to distinguish separate tracks and are not representative of any other characteristics).....	41
<b>Figure 14:</b> MATLAB plot displaying the thresholding process for runs and tumbles. Left: representation of runs and tumbles for a particular track (yellow: incomplete, so disregarded, Red: runs, Blue: tumbles). Right: (Red: runs, Blue: tumbles, Black: incomplete), Top-Right: Change in angle of the pole over time, Bottom-Right: Change in speed over time. ....	42
<b>Figure 15:</b> Track data from cells $3\mu\text{m}$ long ( $\pm 1\mu\text{m}$ ), representing the normal length ranges of E. coli cells (Legends: n= number of individual data points, $\mu$ =mean value, $\sigma$ =variance). Top Left: observed run times (seconds); Top Right: observed run speeds (micrometres/second); Bottom Left: observed tumble times (seconds); Bottom Right: observed tumble angles (degrees). ....	43
<b>Figure 16:</b> Track data from filamentous E. coli cells $10\mu\text{m}$ long ( $\pm 1\mu\text{m}$ ), (Legends: n= number of individual data points, $\mu$ =mean value, $\sigma$ =variance). Top Left: observed run times (seconds); Top Right: observed run speeds (micrometres/second); Bottom Left: observed tumble times (seconds); Bottom Right: observed tumble angles (degrees).44	44

**Figure 18:** Frequency of mean cell lengths observed for each ‘run’ analysed. .... 45

**Figure 19:** Frequency of body aspect ratios (length/width) observed for each ‘run’ analysed..... 45

**Figure 20:** Negative correlation observed between the major axial length (micrometres) of the cell and its mean run speed (micrometres per second). Red line denotes the linear regression model ..... 47

**Figure 21:** Observed variations in tumbling events (seconds) are very slightly negatively correlated with increases in cell length (micrometres) Red line denotes the linear regression model. .... 48

**Figure 22:** The change in run speeds as a measure of log body lengths per second (length specific swimming speed) with increasing cell body sizes. Red line denotes the linear regression model. .... 49

**Figure 23:** Trajectories of multiple E. coli cells tracked using digital holography (Molaei et al., 2014). .... 57

## Abstract

Many microorganisms from all domains of life invest large quantities of energy on locomotion. Adopting a motile lifestyle, although energetically costly, increases the likelihood of encounters with food and nutrients, and reduces the risks of predation or prolonged contact with toxic environments. Understanding the reasons behind these costly adaptations, and discovering the most economical methods for locomotion at the microscopic scale could generate further understanding of many ecological processes at this scale, including; the mechanics of locomotion, food web dynamics, evolutionary pathways and the fluid mechanics of biological systems. Consequently, this project focuses on using the key laboratory bacterial species *Escherichia coli*, to investigate the effect of changes in body shape (aspect ratio) and size on a variety of movement behaviours.

*E. coli* cells treated with the antibiotic cephalexin grow into filamentous forms. Longer cells were found to swim more slowly than normally shaped cells. Run speed was significantly negatively correlated with increases in cell length ( $F_{1, 8858} = 130.5$ ;  $P < 0.001$ ), with speed decreasing approximately -0.109 micrometres per second for each micrometre increase in cell length. Elongation of the cell was also found to impact up the cell's ability to 'tumble' (re-orientate), with cells  $>10\mu\text{m}$  in length being observed to 'run and reverse', rather than 'run and tumble'. Overall, changes in cell shape significantly altered the motile behaviours of *E. coli* cells.

These results suggest that body shape is essential for the successful locomotion of microorganisms, and further study is needed to uncover the evolutionary purposes behind the diverse array of shapes observed in nature.

## **Acknowledgments**

I would like to offer thanks to the many people who contributed to the completion of this research project. Firstly, I would like to thank Professor Stuart Humphries for his continued advice, support, and patience as my supervisor throughout the project. Further thanks go to Dr Oscar Guadayol-Roig for teaching me how to successfully culture the organisms, for writing countless drafts of the MATLAB code used within my analysis and for his guidance throughout the entire experimental and analysis processes. Furthermore, I am grateful to Dr Michael Orchard for his continual support and tolerance, and for supplying copious amounts of coffee. Finally, special thanks goes to the entire Physical Ecology Lab Group; for answering all my questions, helping out wherever possible and providing very interesting scientific debates.

**Chapter 1:**  
**General Introduction**

# **1.0. Introduction**

## **1.1. Size in nature – from the macroscopic to the microscopic world**

Naturally occurring organisms span a size range of over eight orders of magnitude; from the largest mammal, a blue whale (*Balaenoptera musculus*); approximately 30 metres long, to the smallest bacteria (*Nanobacterium sanguineum*); only 200 nanometres in length (Shulz & Jorgensen, 2001). With either end of the size spectrum occurring within the marine environment, it is understandable that aquatic organisms found at the ends of this scale, experience the fluid around themselves in very different ways. Larger organisms (> 1mm) encounter a world dominated by inertial forces, whereas microscopic organisms (< 1mm) are subjected to a more viscous environment. The ratio of these forces (viscous/inertial) affecting the fluid flow experienced by an object or organism is often summarised in terms of a Reynolds number. The Reynolds number (*Re*) is a dimensionless scaling factor that was first introduced by Osborn Reynolds (1883); the value of which can be calculated using equation 1:

*Equation 1*

$$Re = \frac{\rho l U}{\mu}$$

Whereby: *l* is the characteristic length of the object; the length most likely to affect fluid movement (usually the largest axial length of an object facing the direction of flow), *U* is the velocity of the fluid moving around a stationary object, or the velocity of an object moving within a motionless fluid. *μ* is the dynamic viscosity of the fluid and *ρ* is the density of that fluid.

At  $Re > 1$ , inertia is the dominant force and turbulent flows are experienced. In turbulent fluids, although smooth flows often appear to be observed on a larger scale, the individual particles that form the fluid move in a highly irregular manner. As velocity increases (leading to an increase in the  $Re$ ) flows become less stable, resulting in the creation of vortices and eddies which mix the fluid, making it non-reversible (Reynolds, 1883; Vogel, 1994). In comparison, at  $Re < 1$ , laminar flow is present due to an increase in the relative importance of viscous forces. Viscosity is a measure of the ‘stickiness’ of a fluid, calculated as the amount of force required (per unit area) to deform (shear) that fluid. This deformation occurs as a result of the ‘no slip condition’, the fluid particles directly in contact with a surface are unable to move, therefore, any movement of that surface results in the surrounding fluid shearing (Denny, 1993). Fluid moving in laminar flow occurs at much slower rates than in turbulent flows, with the fluid particles moving in smooth paths with almost no mixing (Vogel, 1994). Consequently, fluid flow at this scale becomes reversible, with reciprocal motions returning disturbed fluid particles to their original starting positions.

Aquatic macro-organisms (those easily visible by the human eye; approximately  $\geq 1\text{mm}$ ) experience the fluid around themselves in roughly the same way as a human would. Inertial forces are dominant at this scale (Figure 1); resulting in the need for organisms to generate thrust and reduce drag in order to successfully propel themselves through the liquid medium (Vogel, 1994). Furthermore, if a motile macro-organism were to abruptly halt its swimming effort, the animal would continue to be propelled through the fluid for several body lengths as a result of these inertial forces (Nachtigall, 1981). In an effort to maximise the effects of inertia and minimise levels of drag, the fastest aquatic swimmers have adapted smooth, streamlined body shapes that are elongated and tapered at either end (e.g. whales, dolphins, and mackerel), (Lighthill, 1969). Streamlining

encourages the fluid to flow around an object (or organism) causing a deceleration in the flow rate as the fluid nears the end of the object. This prolongs the duration of time the fluid remains attached to the object, creating a reduction in the  $Re$  as the fluid leaves the object, consequently, reducing drag and preventing the formation of eddies. This results in an increase in the overall speed per unit effort of the organism, and an intensification of the previously mentioned inertial effects (Vogel, 2002). In addition to streamlining, aquatic macro-organisms have developed several different types of locomotion to ensure effective movement through their environment. These include; drag powered swimming (where thrust is gained by creating drag in the opposite direction to travel, e.g. frog leg kicks), lift based swimming (a paddle-shaped limb or fin is moved backwards through the water, e.g. turtles), body undulations (the bending of the whole or partial body into successive waves, e.g. an eel) and jet propulsion (the expelling of rapid jets of water in the opposite direction to travel, e.g. squid), (McNeill, 2002). Each of these methods, in their simplest form, moves a portion of the surrounding fluid to the rear of the organism, increasing the momentum of this unit of fluid, to generate forward propulsion. Due to the non-reversible nature of higher  $Re$  flows, these motions can be repeated in a reciprocal and asymmetric manner, transporting a new section of the fluid with each movement cycle.

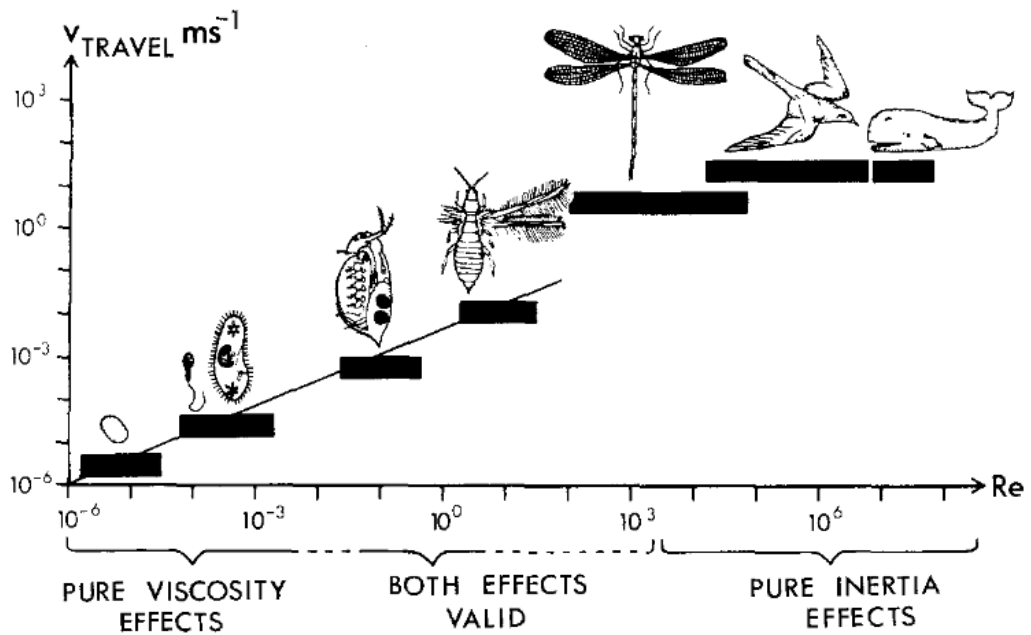


**Figure 1:** Comparison of Reynolds numbers for different organisms with increasing size, highlighting the dominant forces present at each scale (From Nachtigall, 1981).

Within low  $Re$  regimes ( $Re < 1$ ), the relative effect of viscosity is considerably increased and reciprocal locomotion becomes ineffective. Higher viscosities result in the reduction of inertial forces, therefore, when a unit of fluid is moved forwards as a result of powered swimming, the fluid stops moving almost immediately after the swimming effort is removed. Consequently, if an object was to move forwards then backwards (like a paddle or turtle limb) the same unit fluid would move with the object, both forwards and backwards, returning to its original position at the end of the movement cycle, thus preventing any forward propulsion (Purcell, 1977). Consequently, microscopic organisms; such as bacteria and plankton, have developed locomotion through cyclic motions which utilize two or more degrees of freedom rather than the inefficient reciprocal motions used in higher  $Re$  regimes. Microscopic organisms generate movement via the rotational motion of long, thin appendages; either cilia or flagella. Flagella typically occur at greater lengths and in fewer numbers than cilia;

moving via a rotary, helical (corkscrew) motion (prokaryotes) or via undulatory sinusoidal waves (eukaryotes), either individually, or within a co-ordinated motion. Whereas cilia typically beat from left to right, with a powerful main stroke that offers the propulsive force and a returning recovery stroke which minimises drag (Denny, 1993; Vogel, 2008). To enable the cell to travel at a constant speed, the total amount of thrust produced by the ciliary or flagellar appendages must be equal to the amount of viscous drag acting upon the cell as a whole (Sleigh, 1991).

The earliest studies of movement at these microscopic scales were undertaken by Anton Van Leeuwenhoek (1702), who described the abundance of life within a single water droplet. He labelled the tiny life forms which he observed as ‘animalcules’ and described the movement of several of these microscopic organisms in great detail; ‘each had their different motion’ ‘swimming in circles thro the water’. His descriptions (the first of many to follow) detailed the variations in types of locomotion across a range of microorganisms swimming at high viscosities. In more recent years, the movement of organisms living in low  $Re$  regimes, including numerous species of; zooplankton, phytoplankton, and bacteria, has become a topic of varied scientific interest, with many studies exploring both the physiological adaptations and motile behaviours of numerous species of microscopic organisms (useful reviews include; Brennen & Winet, 1977; Jarrell & McBride, 2008; Guasto *et al.*, 2012). This study aims to focus specifically on the motility within the bacterial domain of life, the primary focus being on the fundamental experimental species: *Escherichia coli*.

## 1.2. The Relationship between Size and Motility in Bacteria

Bacteria are single-celled prokaryotic organisms that range in size from 0.2 $\mu\text{m}$  (*Mycoplasma pneumoniae*) to 750 $\mu\text{m}$  (*Thiomargarita namibiensis*), and are highly dependent on the diffusion of nutrients from surrounding fluids for their growth and development (Schulz & Barker-Jorgensen, 2001). Swimming in larger species can augment this necessary diffusion by raising the Péclet number (a dimensionless ratio representing the importance of advection with respect to diffusion) above the level of unity (a value of one), to instigate a higher rate of delivery (via advection) than is possible from diffusion alone (Vogel, 1994). However, for a single cell of *E. coli* to increase its rate of nutrient uptake by as little as 10% it would have to swim approximately 20 times faster than its normal linear speed (Purcell, 1977). As a result of this, the majority of motile bacteria are unable to swim fast enough to increase their own food supply above the level achieved through diffusion alone (Dusenbury, 2009). Consequently, the main purpose for cell motility must be to re-orientate towards areas of increased or more beneficial nutrient compositions, and away from areas where the nutrients have become depleted or which contain toxic substances (Purcell, 1977). In order to do this effectively, the individual cell must use chemical sensors (chemoreceptors) located on the cell membrane, to detect nutritional gradients and swim faster than the rate of nutrient diffusion through the surrounding fluid to be able to track and utilize a nutrient flux (Mitchell & Kogure, 2006).

Cell size affects the efficiency of both motility and the diffusion of nutrients into and out of single-celled organisms. Nearly every organism on earth (irrespective of size) swims at a speed on the order of ten body lengths per second (Berg, 2004), therefore, larger unicellular organisms are often able to travel greater distances within a given time period, than their smaller counterparts. However, for a given shape increased cell

volume lowers the surface to volume ratio, thus both lowering the relative space on a cell's surface for diffusion sites and increasing the length of the internal diffusion pathway (Koch, 1996). Consequently, any nutrients absorbed by the cell take longer to diffuse to the required location(s) within that cell. Therefore, there is an upper limit for cell size at the point where internal nutrient transportation can still function at an adequate rate to fuel a cell's metabolism. It is estimated that cells larger than 800 $\mu\text{m}$  in diameter would be unable to absorb nutrients at a rate equal to or faster than the rate of consumption by the cell, without resorting to other feeding strategies (Dusenbery, 2009).

Dusenbery (1997) predicted that there would also be a minimum size limit of 0.3-0.6 $\mu\text{m}$  in diameter, for locomotion to have a beneficial effect on the organism. However, this value is highly dependent upon the physical constraints of the organism's natural habitat. In areas of continuously poor nutrient concentrations, the benefits of being small far outweigh the motility cost of a reduction in the net relative distance travelled by smaller cells, as the higher surface-to-volume ratio reduces the cell's internal diffusion pathway and increases the number of chemoreceptors per unit volume of the cell, enabling more efficient utilization of the available nutrients than in larger cells (Mitchell, 2002). Conversely, in nutrient loaded environments, smaller cells are unable to effectively move away from diminished nutrient patches created by their rapid rate of nutrient consumption, and due to their lower net movement over a given time period. Therefore, in higher nutrient concentration conditions, an increase in cell size and its associated increase in speed become more advantageous, enabling larger motile cells to move away from depleted areas into new areas more efficiently than their smaller counterparts (Mitchell, 2002).

Allometric scaling relationships have been associated with many aspects of anatomical and physiological attributes of a wide variety of organisms, spanning multiple orders of magnitude. However, to date, little correlation has been found to suggest a direct link between cell size and cell motility in single-celled micro-organisms (Brown & West, 2000). This may be due, in part, to the small number of species studied, but also the variety of ecological niches that the test species naturally inhabit (Crawford, 1992 & Johansen *et al.*, 2002). Vogel (2008) plotted swimming speed data from previous studies (Brennen and Winet, 1977 & Mitchell *et al.*, 1995), as a function of body length; revealing a slight tendency towards larger cells being slower than smaller individuals on a relative scale (Figure 2). However, this is only a small subset of the wide variety of micro-swimmers observed in nature, and represents individuals covering a range of motility structures, swimming patterns, ecological niches, body sizes and shapes.

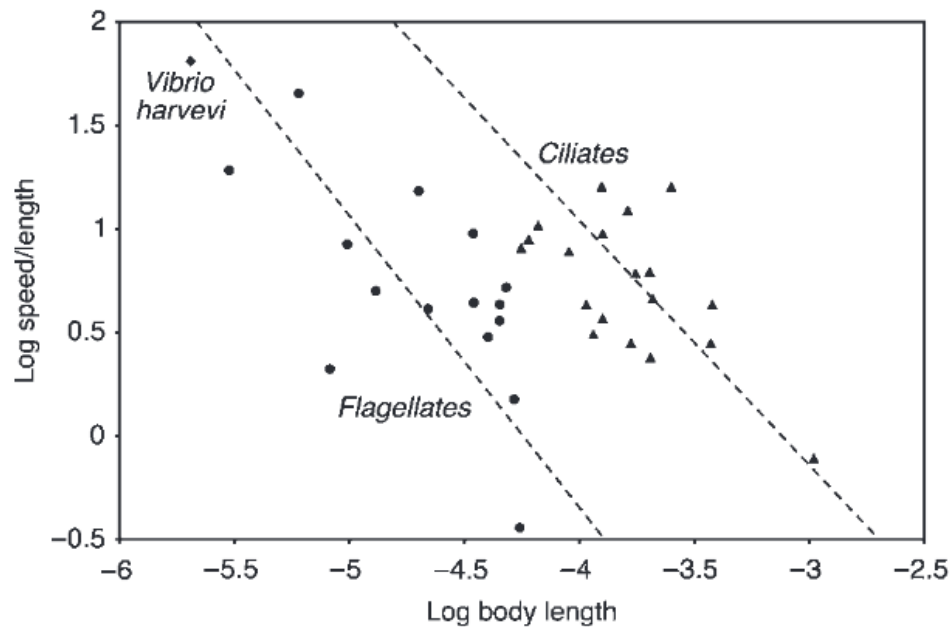


**Figure 2:** Body length plotted against swimming speed as a measure of body lengths per second for a variety of micro-organisms. Circular markers denote the flagellated species, the triangular markers denote the ciliates, and the diamond marker denotes the bacterial species *Vibrio harvevi* (Vogel, 2008).

### 1.3. Motile Cell Shape

When considering bacterial motility, cell shape is highly influential in helping to determine the maximum speeds and efficiency at which a cell can move through the surrounding fluid (Young, 2007). The majority of motile cells have elongated/rod-shaped bodies, with only 10% of motile bacterial genera exhibiting spherical (cocci) forms (Dusenbery, 2009). Rod-shaped cells are thought to be the first bacterial shape to have arisen from an evolutionary perspective, with cocci being a derivative of the initial rod shape (Young, 2007). Elongation of a cell appears to have a number of advantages for movement within a liquid environment. Firstly, increasing the axial length of a cell has been shown to reduce its sinking rate, thus optimizing the time spent near the surface of the water, in areas of higher nutrient and oxygen concentrations (Dusenbery, 1998). Rod shapes also generate less frictional resistance than spherical cells of the same volume, when moving through surrounding fluid. Furthermore, it has been suggested that highly efficient rod shapes can move up to five times more easily than spherical counterparts of the same volume or mass (Young, 2006). Finally, rod shapes are also believed to enable superior chemotactic responses than those observed within spherical cells (Dusenbery, 2009). It is estimated that rod shaped bacteria have the ability to measure changes within the chemical gradient 650 times more accurately than cocci cells, due mainly to the significant reduction in rotational displacement by Brownian Motion (Young, 2006; Dusenbery, 2009).

Wild-type *E. coli* cells are rod-shaped, with a length-to-width ratio of approximately 3.7, which is almost identical to the optimal shape suggested by Cooper and Denny (1997) to provide the cell with the most efficient shape to move through the fluid environment using the least amount of force. However, Dusenbery (2009) argued that the optimal aspect ratio for increased swimming efficiency would be less than 2 (1.952), yet this is

not representative of observations in nature, as the median axial ratio observed within swimming bacterial species is above 3. To date there has been little research into the importance of cell shape across the huge range of single celled microorganisms currently known to science. The diverse array of forms observed within nature (Figure 3), suggest that shape plays some key role in the success of microorganisms (Young, 2007).

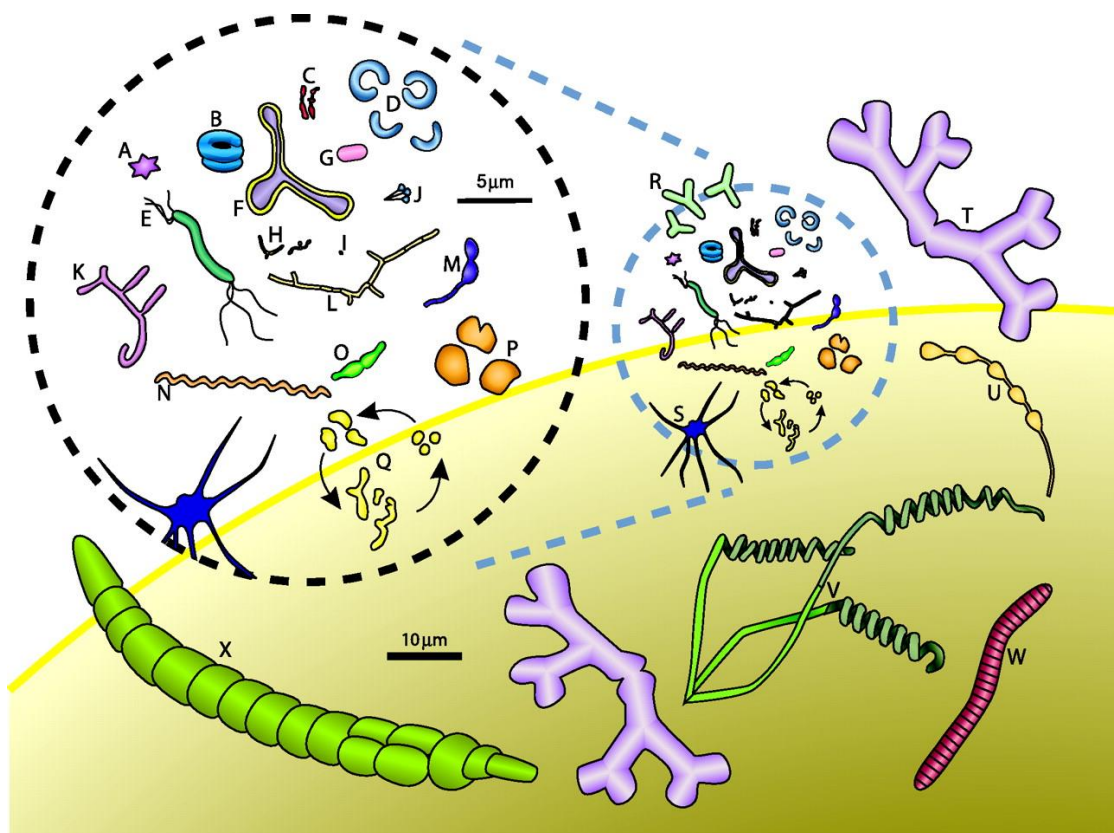


**Figure 3:** Examples of the diverse array of prokaryotic shapes currently recorded (From Young, 2006).

All cells are drawn to scale, colours are for emphasis only.

#### 1.4. Mechanisms for Motility

Many bacterial cells attain forward propulsion through the rotation of one or more flagella filaments. Flagella are long, thin appendages attached to the membrane of the cell, and comprised of Flg and Fli proteins (Berg, 2003). Prokaryotic cells have flagella filaments which are cylindrical and rigid, with a helical form. The individual flagella filaments are each attached to a reversible rotary motor located within the cell membrane, via a flexible hook. Each filament is rigid and comprised of single polypeptide chains of the protein flagellin (Fli.C) (Berg, 2003), (Figure 4). The rotary motor of bacterial cells is powered by the movement of ions or protons along an electrochemical gradient. In many marine bacteria this is created by the movement of calcium ions, however, in the case of *E. coli*, the motor power is generated by the movement of protons down the electrochemical gradient (Berg, 2003). This rotary motor drives the base of the flagellum, controlling both rotation direction and rate; based upon specific chemical cues received from the surrounding environment (Silverman & Simon, 1974). The primary direction of rotation is dependent upon the handedness of the spiral, as the aim of the motion is for the helical waveform to propagate outwards, and as such generate a 'pushing' motion (e.g. left-handed forms generally rotate counter-clockwise), (Figure 5), (Sleigh, 1991). However, during periods of motor reversal, as a means of re-orientating the cell, the wave propagates inwards towards the cell body, often resulting in the intertwining of several of the individual filaments (Macnab, 1977).

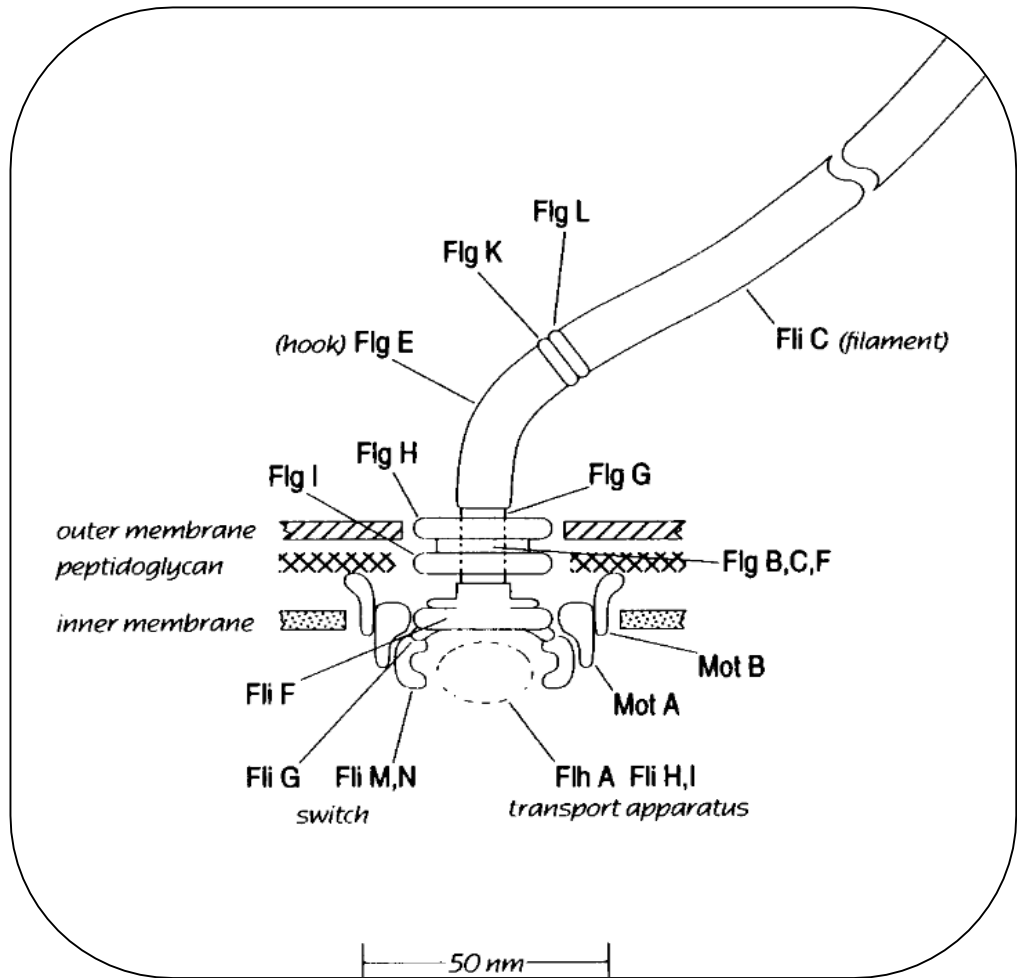


**Figure 4:** Structure of a single bacterial flagellum. Figure highlights the position of each of the Flg and Fli proteins, and the general structure of the organelle (From Berg, 2003).

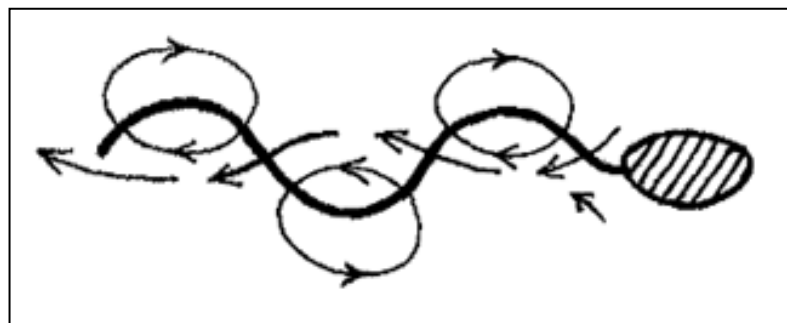


**Figure 5:** Model swimming cell; arrows denote the direction of fluid flow generated by a singular rotating flagellum (From Sleight, 1991).

Swimmers propelled by flagella can be categorized as either ‘pushers’ or ‘pullers’. *E. coli*, like many other bacteria, can be considered ‘pushers’ as they push fluid away from the poles of the cell. This causes fluid to move inwards at the centre of the axial length of the cell creating a force exerted forwards by the body of the cell, and backwards by the flagellum. The movement of fluid (fluid flow-field) surrounding swimming organisms driven by a single flagella bundle can be considered as a stokeslet – a theoretical single point of force (Flores *et al.* 2005). For a cell moving in this manner, to travel at a constant speed the total level of thrust produced by the flagella bundle must equal the level of viscous drag acting upon the cell (Sleigh, 1991).

### 1.5. The Random Walk Model

All micro-organisms moving through a fluid medium are subject to the rotational forces created by Brownian motion. Brownian motion is the random migration of particles as a result of thermal energy, first observed by Robert Brown in 1827, and later linked to the kinetic theory of matter in 1905 by Albert Einstein (Kac, 1947). The thermally driven movement of particles is impeded by frequent collisions between individual particles; the higher the density of particles, the greater the frequency of these collisions. With each collision, the affected particles are re-orientated towards a new direction, the observed effect of which has been termed the ‘Random Walk’ of a cell (Berg, 1983). Brownian motion creates an average rotational displacement of approximately 30 degrees about a random axis, and the translocation of a particle in any random direction of roughly 1 $\mu$ m/s (Berg, 2004). However, the extent of these effects varies, as the amount of displacement is inversely proportional to a cell’s size and velocity (Schulz & Barker-Jorgensen, 2001). At diameters of less than 0.6 $\mu$ m Dusenbury (1997) predicted that cells would be unable to bias this ‘random walk’ through the use of their own

motility mechanisms, and directional movement would become impossible. This value is supported by the fact that the smallest motile bacterium recorded to date; is 0.8 $\mu\text{m}$  in diameter, with all smaller species belonging to non-motile genera (Dusenbury, 1997).

## 1.6. Ballistic and Diffusive Movement

The movement paths of all microscopic organisms can be defined as either ballistic or diffusive, using the continuous random walk model described in the formative work by Taylor (1922). Ballistic movement is defined by straight path types which do not back-track over previously covered areas, thus the total distance travelled by a cell is equivalent to the net movement in any particular direction (Scheuch & Menden-Deuer, 2014). Ballistic movement is generally exhibited by larger, predatory planktonic organisms, as straighter path types increase the swimming area covered, and as such, increase the likelihood of encounter rates between prey items and potential mates (Visser & Kiorboe, 2006).

In comparison, diffusive movement incites more convoluted path types and is representative of the 'random walk' associated with many bacterial species. The short chemotactic 'memory' and Brownian displacements linked to bacterial movement, confines many micro-organisms to tortuous path types, which often revisit previously explored territory (Berg, 2000; Codling *et al.*, 2008). Diffusive movement is indirect and has a small mean squared dispersal distance (MSDD), resulting in the organism displaying behaviour close to that predicted for the random walk model, thus only slight net movements in a chosen direction are exhibited (Kareiva & Shigesada, 1983; Codling *et al.*, 2008). Various studies on *E. coli* suggest that it has an effective diffusivity of

between  $7.0 \times 10^{-1} \mu\text{m}^2/\text{s}$  and  $8.7 \times 10^{-3} \mu\text{m}^2/\text{s}$  dependent upon temperature and strain/type (Kim, 1995).

## 1.7. Study Species

### 1.7.1. Bacterial Strain

*Escherichia coli* are common enteric bacteria, naturally found in the lower intestine of endothermic organisms. As a result of large availability and easy of culture, they have been heavily studied and are now considered a model species for experimentation. The strain of *E. coli* used for these experiments was the wild-type AW405, a derivative of the K-12 strain which originated from Lederberg's W2580 strain (Armstrong *et al.*, 1956). AW405 was selected because of its known high motility levels in comparison with some other *E. coli* strains and frequent use in motility and chemotactic studies (e.g. Adler *et al.*, 1967; Mesibov & Adler, 1972; Berg & Turner, 1979; Segall *et al.*, 1985). AW405 has successfully been used in a variety of shape alteration experiments, and has been shown to retain both motility and chemotactic responses in elongated forms (Ishihara *et al.*, 1983; Maki *et al.*, 2000; Takeuchi *et al.*, 2005). The culture was purchased from NCIMB specialist microbial and chemical services (NCIMB Ltd, Ferguson Building, Craibstone Estate, Bucksburn, Aberdeen) and was received freeze-dried, before initial growth on Agar (Melford Laboratories Ltd, UK; prepared as directed by manufacturer) plates, followed by regrowth in LB broth (Melford Laboratories Ltd, UK; diluted according to manufacturer's instructions to 25g/l). The liquid cultures were aliquoted into 1ml eppendorf tubes before being frozen at  $-70^\circ\text{C}$ ; these frozen stock cultures were then used as isolates to initiate all experiments.

### 1.7.2. Cell Culture

Before experimentation, cells were thawed and resuscitated in Minimal Growth Media (MGM) in an attempt to maximise motility levels (Maki *et al.*, 2000). The media was prepared as detailed by Vogel and Bonner (1956) through the addition of; Magnesium Sulphate Heptahydrate, Citric Acid Monohydrate, Potassium Phosphate Dibasic and Ammonium Sodium Phosphate Dibasic Tetrahydrate (all purchased from Sigma-Aldrich Co., UK), to deionised (DI) water. The media solution was then autoclaved on a liquid cycle, before the addition of specific nutrients for *E. coli* wild-type AW405; Sodium DL-Lactate, L-Histidine, L-Leucine, and L-Threonine (Mesibov & Adler, 1972) (All purchased from Duchefa Biochemie B.V, Netherlands; except Sodium DL-Lactate which was received from Sigma-Aldrich Co., UK). After thawing, 0.5ml of sample bacteria were added to 24.5ml of MGM and grown overnight at 33°C in an incubator and rotary shaker (New Brunswick Scientific Innova 44) at 200 rpm.

### 1.8. Escherichia coli Movement

*E. coli* form rod-shaped cells that are approximately 800nm wide and 1.5µm long. The cells are peritrichous (have randomly distributed flagella along their body), with each having approximately 8 to 10 flagella filaments arranged in a left-handed helix, that rotate synchronously (at a rate of approximately 270 rotations per second) in a counter-clockwise direction (CCW) to form a bundle at one pole of the cell (Kudo *et al.*, 1990; Berg, 1996). This flagellar bundle is highly advantageous, as it acts as a single propeller generating more thrust, but almost identical levels of drag, than an individual filament (Magariyama *et al.*, 2001). Bundle formation is also useful in the reduction of rotational movement due to Brownian Motion, increasing the accuracy of the cell's directionality. In *E. coli* cells, this stabilization equates to a 3-10% reduction in the

random rotational movement created by Brownian motion (Mitchell, 1991). However, the rapid rotational movement of the flagella also generates torque, which the cell combats by rotating its body in the opposite direction to the flagellum, ensuring accurate forward propulsion (Berg, 2004). As the cell speed increases, the level of torque produced decreases in a linear manner, suggesting that maintaining faster cell speeds is advantageous for reducing both body rotations and flagellum motor effort (Lowe *et al.*, 1987).

*E. coli* move at a rate of approximately 14µm/s by a series of straight ‘runs’ and re-orientating ‘tumbles’ (Previously known as ‘twiddles’ (Berg & Brown, 1972)) (Figure 6). When the flagella motors work in unison, turning in a CCW direction, the cell moves in a linear path and is said to be ‘running’. Each ‘run’ phase lasts approximately one second, compared with a much shorter ‘tumble’ time of approximately 0.2 seconds (Berg & Brown, 1972). A ‘tumble’ occurs when one or more of the flagellar motors reverse their direction, resulting in the affected filaments turning in a clockwise (CW) direction (Turner *et al.*, 2000). During the CW rotation of the flagellum, the individual filament(s) form more tightly wound (curled) helical structure(s), roughly half the pitch of their usual formation (Berg, 2003). This alternate form, coupled with the flagellar motor reversal, provides the negative wave propagation required for the cell to ‘tumble’; rotating rapidly in a random direction (Macnab & Ornston, 1977). A ‘run’ phase only returns when the reversed filament reverts back to the CCW direction, uncurls and re-joins the bundle. The cell is then moving in a new, random direction (Figure 7), (Darnton *et al.*, 2006). This continuous cycle of ‘run’ and ‘tumble’ behaviours enable the cell to orientate towards areas of more favourable conditions, as the cell is unable to consciously ‘steer’ towards positive environmental cues. By increasing the duration of

runs during positive conditions, and increasing tumbles during negative conditions, the cell increases its chances of following valuable chemical gradients.

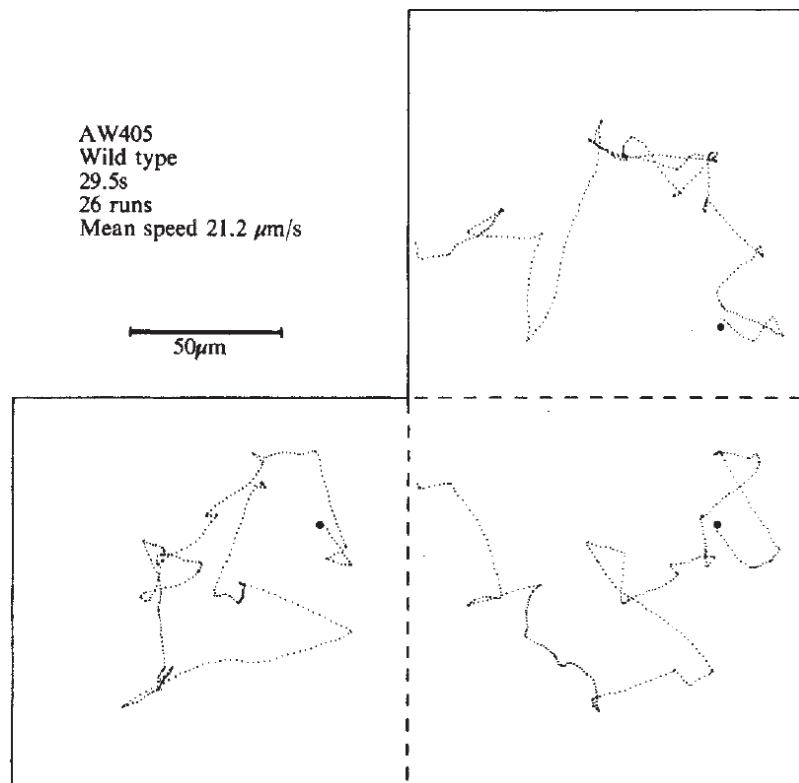


**Figure 6:** A typical track following the random movement of 'runs' and 'tumbles' of a single *E. coli* cell, produced using a custom-built tracking microscope (From Berg & Brown, 1972).

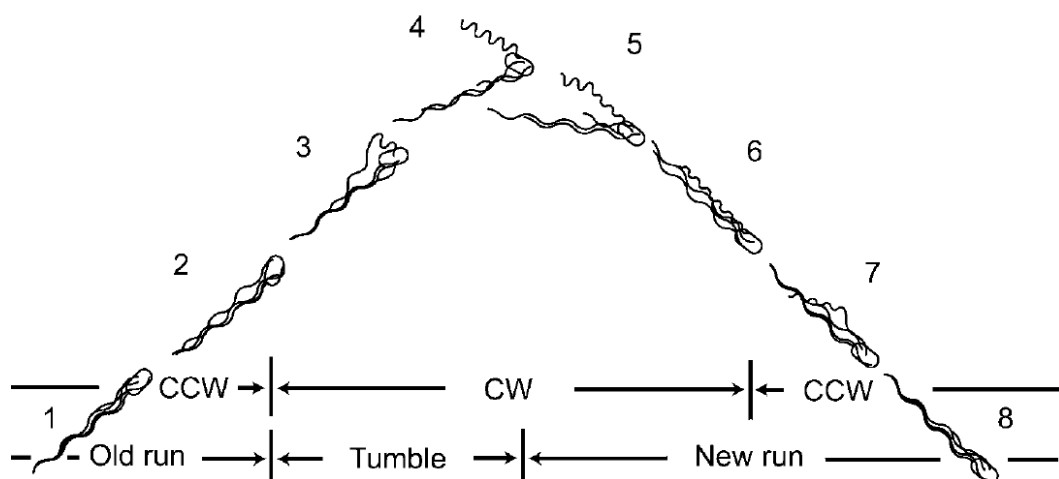


**Figure 7:** An example of *E. coli* flagella movements during one complete run-tumble cycle (From Darnton *et al.*, 2006). By the end of the tumbling period (stage 4), the reversed flagellum has become tightly curled and the cell has re-orientated into a new directionality of movement.

## 1.9. Project Aims

Very little is known about the importance of microbial shape (Young, 2006). Single celled microorganisms have a range of forms; from simple coccoid and rod shapes, to more complicated spirals, stars and even squares. Many of these differing forms expend large percentages of their metabolic energy synthesizing motility structures and generating the power required to move (Dusenbery 1998; Mitchel, 2002). By focusing experimentation on a single species (in this case the well characterised experimental bacterium *E. coli*) observed changes in behavioural responses can be directly linked to alterations in body size and shape. Motility differences which could be linked to ecological and structural differences between differing species can be controlled for, and an optimal shape for powered locomotion in low Reynolds environments can be hypothesised.

The main goal of this study is to characterise individual cell motility in filamentous forms of *E. coli*. Particular focus will be placed upon the comparison of the key components of bacterial motility at varying axial lengths. The changes in aspect ratio are expected to create alterations in the iconic ‘run’ and ‘tumble’ behavioural patterns, as well as overall speeds and directionality. The key aims of this study include:

- To determine changes in run speed with increasing cell length.
- To locate changes in tumble frequency and magnitude (angle) at differing sizes.
- To observe any alterations in the swimming behaviour of filamentous cells.
- To identify the minimum size at which the force produced by motor reversal produces an insufficient force to generate the tumbling behavioural response.
- To identify an optimal size for cell movement.

## **Chapter 2:**

# **Experimental Chapter: The Effect of Changes in Cell Aspect Ratio on Locomotory Behaviours**

## **2.0. The Effect of Changes in Cell Aspect Ratio on Locomotory Behaviours**

### **2.1. Introduction**

Single celled microorganisms require stability in their shape to control necessary biological processes such as cell division, polarisation and motility. Within eukaryotic cells, a cytoskeleton created by actin filaments is the main structural component used to maintain a controlled cellular shape (Fletcher & Mullins, 2010). However, as most prokaryotes lack internal actin filaments and a structural cell wall, the ability of bacteria to maintain the wide variety of shapes observed in nature was, until recently, largely unexplained. Schwarz and Leutgeb (1971) established that this essential cell stability was a result of morphogenetic structures within the cytoplasmic membrane rather than a specific chemical composition within the cell. However, it was later revealed that these structures are formed by the protein MreB (found in the Murein Cluster E gene cluster), which produces helical actin-like filaments that span the entire longitudinal axis of the cell (Figure 8), providing rigidity and enabling the stabilization of a particular cellular diameter (Doi *et al.*, 1988; Shih *et al.*, 2003). The cytoskeleton produced by these filaments is comparable to that found within eukaryote cell walls, and generates a similar level of stiffness to that of the peptidoglycan chains observed in eukaryotic cells (Wang *et al.*, 2009). Furthermore, the MreB proteins are thought to be homologous to the actin found in eukaryotic cells; biochemical and structural similarities between the two proteins suggest that they both arose from an early common ancestor (van den Ent & Löwe, 2001; Doolittle & York, 2002).

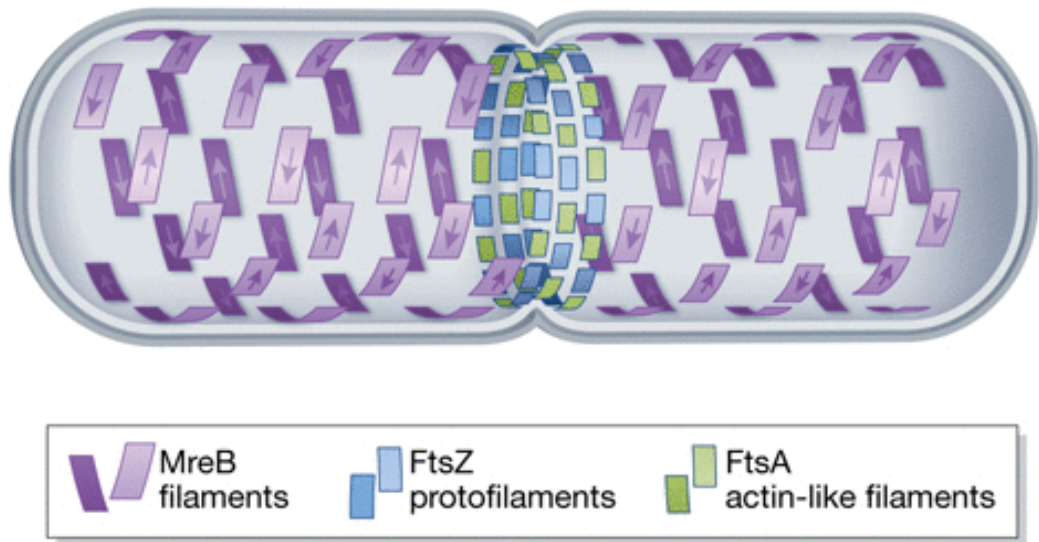


**Figure 8:** Cell wall structure of rod-shaped prokaryotes. The purple patches forming a helical pattern are the actin-like filaments (MreB) which give the cell its rod structure. The blue and green patches in the centre of the cell are the FtsZ and FtsA filaments involved in cell division (Juarez & Margolin, 2012).

### 2.1.1 Antibiotic Treatments

MreB proteins are restricted to the major axial length of the cell, to enable cell division to occur at the poles. In cells of *E. coli*, natural cell division occurs when the protein FtsZ (Figure 8) moves to the centre of the cell to form the Z-ring. This Z-ring facilitates the binding of other division proteins to create a division septum. The septum constricts, pulling the cytoplasmic membrane inwards, resulting in the creation of a dividing wall in the centre of the cell, thus producing two daughter cells (Weiss, 2004) (Figure 9).

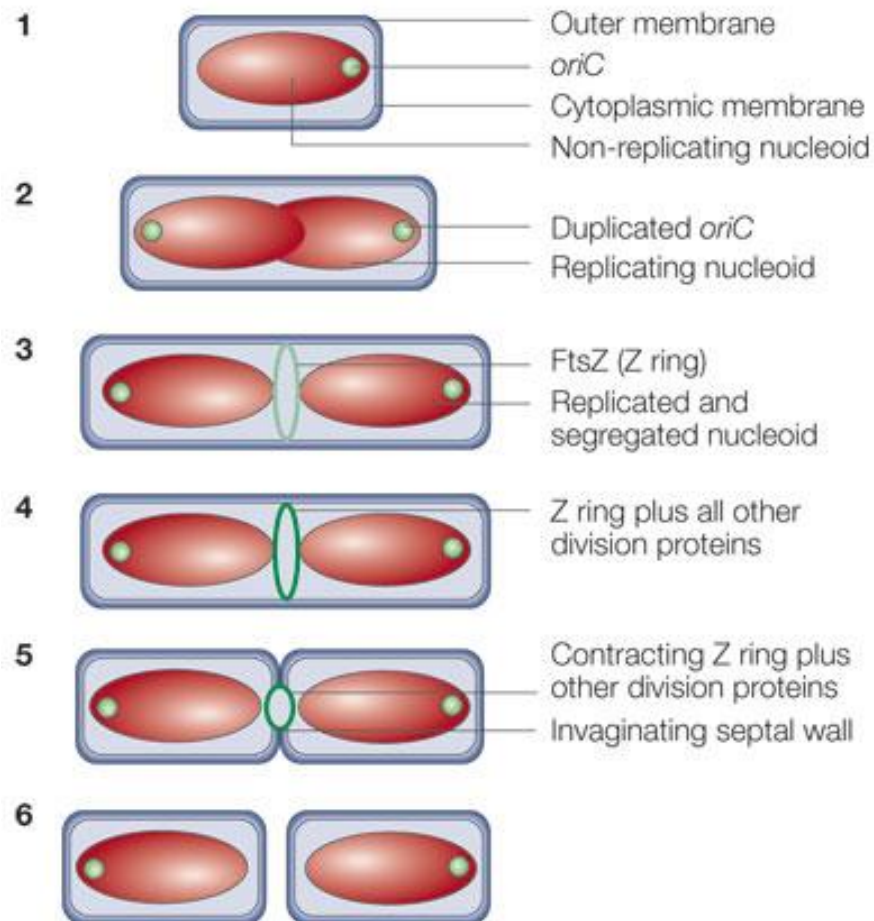


**Figure 9:** The various stages of natural prokaryotic cell division, highlighting the role of the FtsZ protein (Z-Ring) in the division process (Margolin, 2005).

Cephalexin is a  $\beta$ -lactam antibiotic which, when added to cultures of *E. coli*, has been shown to cause the filamentation of cells, without otherwise altering their growth patterns (Greenwood and O’Grady, 1973a). Cephalexin, unlike many other  $\beta$ -lactam antibiotics, specifically targets the FtsZ protein, inhibiting the synthesis of a Z-Ring (cross walls) within the cell and preventing the division process without affecting other structural aspects of the cell (Spratt, 1975; Greenwood and O’Grady, 1973a). Since the side walls of the cell remain intact the cell continues to grow, without dividing, into an elongated ‘snake-like’ form (Figure 10). These elongated cells have been recorded at lengths of up to 50 times larger than that of an untreated cell (Maki *et al.*, 2000). Furthermore, if the dose of Cephalexin remains close to the M.I.C. (Minimum

Inhibitory Concentration) of approximately 10-200 $\mu$ g/ml (Goodell *et al.*, 1976; Rolinson, 1980), and is added during the mid-to-late logarithmic phase, the *E. coli* cells do not lyse at a rate different to that of untreated cells (Greenwood and O'Grady, 1973b). Consequently, Cephalexin can (unlike many other Cephalosporins) be used to stop division within bacterial cells without otherwise altering their natural growth and development, resulting in filamentous forms.

### 2.1.2 Filamentous Cells of *Escherichia coli*

Filamentous cells of *E. coli* (Figure 10) remain very poorly understood in comparison to unaltered cells, with very limited research having been undertaken to understand their motile behaviours. Maki *et al.* (2000) noted that cells treated with  $\beta$ -lactam antibiotics develop multiple nucleotides and continue to synthesize flagella across the length of their body. These flagella do not rotate synchronously, creating the bundle formation, as untreated cells do. Instead, for filamentous cells, only those flagella closest to one another move in unison, suggesting that the signal controlling the flagella motors is localized and unable to span the entire length of an elongated cell (Ishihara *et al.*, 1983). Moreover, filamentous cells of *E. coli* reach a point where-by the natural movement consisting of 'runs' and 'tumbles' becomes impossible due to their size. The 'tumbling' behavioural response is unable to take place, as the change in direction of a single flagellum does not generate sufficient force to throw the larger cells off balance. Consequently, a number of filamentous cells 'run' and 'stop', rather than changing direction (Maki *et al.*, 2000). The exact size at which this occurs remains unclear.

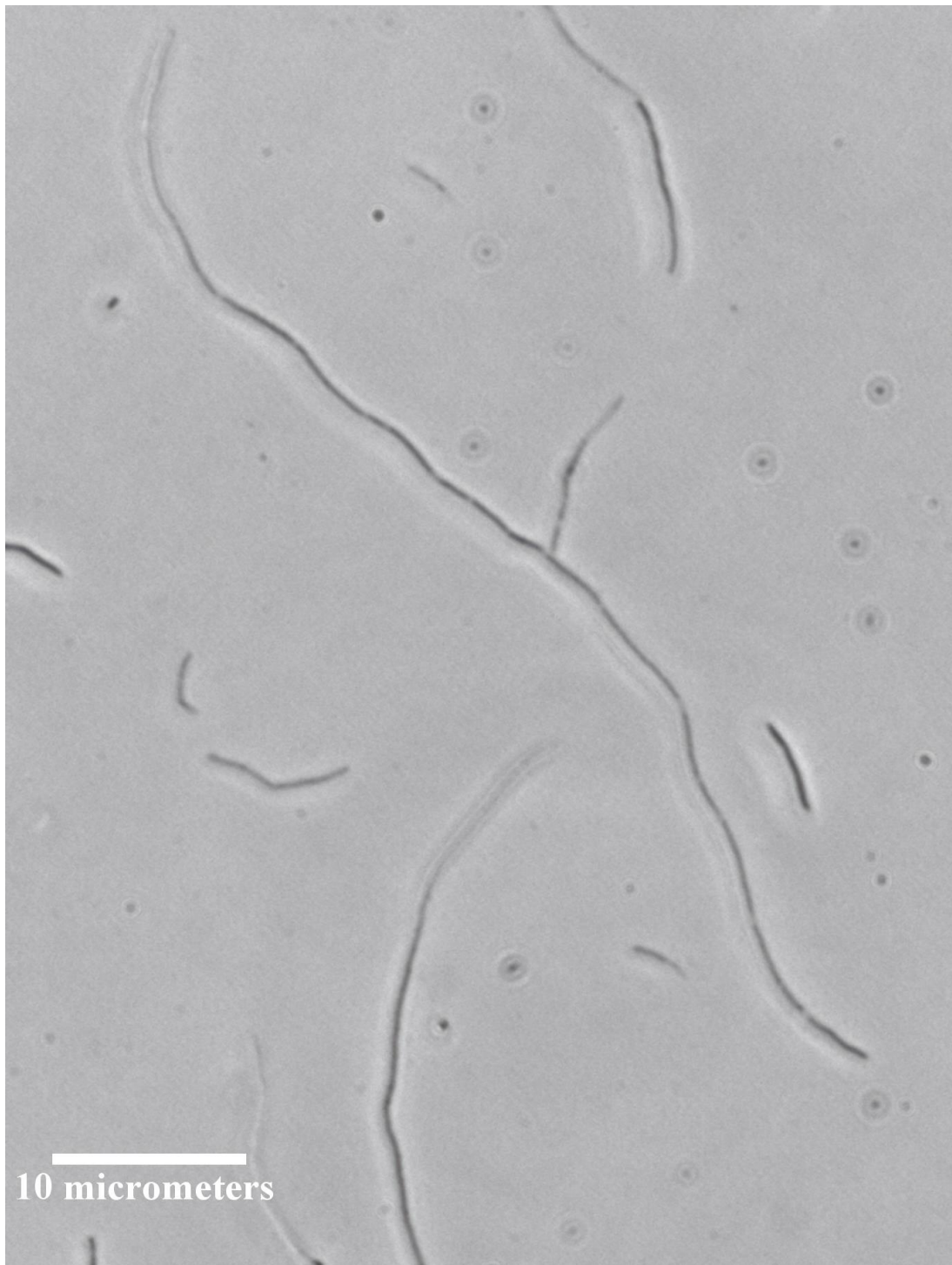


**Figure 10:** Phase contrast microscope image (x1000 magnification) of filamentous *E. coli* cells. Cells treated with cephalixin and incubated for 24 hours to produce maximum lengths of up to 50 micrometres in length.

## 2.2 Methods

### 2.2.1. Cell Preparation

Twenty-four hours after the initial resuscitation of frozen cells in MGM, 0.5ml of the saturated culture was removed from the incubator, and added to two sterile 250ml flasks, each containing 24.5ml of MGM. These daughter cultures were then returned to the rotary shaker for approximately two hours. At this point the optical density of the culture was assessed using a spectrophotometer (ATI Unicam 8625). Optical density (OD) readings at levels above 0.65 absorption (A), when measured with a light beam at the 600nm wavelength ( $OD_{600} \sim 0.65A$ ), indicated that the cells had reached the mid-exponential growth phase, when compared with calibration curves produced prior to experimentation, from the same untreated stock cells. At this point, the cells were inoculated with the antibiotic treatment, as cells within the exponential phase are considered to be the most motile (Adler & Templeton, 1966), and also provided a sufficient optical density for the filming of multiple cells. Absorption readings below 0.65 were returned to the shaker for 30 minutes, before being re-assessed in the spectrophotometer. This process was repeated as necessary until the mid-exponential growth phase had been achieved.

### 2.2.2. Cephalexin Treatment

All cells were treated with the  $\beta$ -lactam antibiotic cephalexin to induce filamentation, through the inhibition of the Ftsz protein (Chapter 2.1.1). Cephalexin hydrate (Sigma-Aldrich) was diluted to 10mg/ml using DI water and extensive vortexing. The resulting antibiotic solution was then filter sterilized (200nm mesh size) and aliquoted into 1ml eppendorfs, before being stored at  $-20^{\circ}C$ . Due to its light sensitivity, cephalexin was

always stored in the dark and all stock solutions of the antibiotics were used within one month of dilution, as advised by the manufacturer's instructions. Before experimentation, cephalexin was removed from the freezer and allowed to thaw naturally for approximately 30 minutes at room temperature. When the experimental cells reached the mid-exponential growth phase ( $OD_{600} \sim 0.65A$ ), 144 $\mu$ l of the 10mg/ml cephalexin solution was added to the remaining 24ml of culture to ensure a dilution of 60 $\mu$ g/ml. Samples from the culture could then be removed at 30 minute intervals for filming, to provide cells of varying axial lengths.

### 2.2.3. Slide Selection

In pilot experiments both cavity and flat slides were used for filming the treated cells using an inverted phase-contrast microscope (Zeiss Axiovert A1). Both types of slide had limitations for their use within the main experiment. Cavity slides (well size  $\approx$ 15mm diameter 0.6mm depth) biased the data towards slower moving cells, as fast cells moved out of the focal plane very rapidly, producing shorter tracks. In comparison, flat slides filmed all of the cells moving within the field of view, but prevented free movement in the z direction. Furthermore, cells close to the boundaries often displayed reduced movement as a result of the increase in 'wall effects' created by close proximity to the solid boundary. Consequently, cavity slides were selected for experimentation, in an attempt to reduce movement constraints. However, due to the filming techniques used, video analysis was limited to two dimensional swimming in the x-y plane. In an attempt to exclude cells which were significantly impeded by close proximity to the glass surface; in experimental footage all cells displaying an average speed below half of the minimum run speed of *E. Coli* AW405 observed by Berg and Brown (1972) (approximately 4  $\mu$ m/s) were disregarded.

#### 2.2.4. Video Acquisition

Before filming microscope slides and cover slips were cleaned with 70% ethanol, rinsed with DI water, and dried using soft tissue. 40µl of the treated *E. coli* culture was placed onto each slide, and examined using an inverted phase-contrast microscope (Zeiss Axiovert A1) at 200X magnification. Phase-contrast microscopy was selected as it provided superior image quality compared with standard bright field techniques due to low refractive index of most bacterial cells. Furthermore, it is a relatively low cost and easy to implement technique, and is preferable to fluorescence microscopy which could artificially manipulate motility responses due to the binding of fluorophores to motility structures. Cells were observed at 33°C on a heated microscope stage, under a bespoke stage incubator to reduce the flows created by convection currents. Video capture was undertaken using a high-speed camera (PixiLINK), which captured live video footage at 30 frames per second (fps), for durations of two minutes per video. Each slide was only used once, as longer timespans led to cells migrating towards the solid boundaries and sticking to both the glass slide and the cover slip, thus restricting natural movement. Furthermore, prolonged exposure to the heated stage led to evaporation of the media, rendering the sample useless. As cell size increased over time, it was advantageous to reduce magnification from the 20x objective lens to the 10x objective lens to increase the area of the field of view (and reduce total magnification to 100x), to increase the number of cells imaged by the video camera. All videos were saved in AVI format and converted to 8 bit grey scale using the open-source software Image J (version 1.48) prior to analysis.

### 2.2.5. Video Analysis

All videos were imported into MATLAB (v. R2013b) for track analysis. The custom designed tracking script used (Guadayol-Roig *et al.*, (in prep)) created a background image from the median pixel intensity of all the frames within the video. This background image was then subtracted from each frame to eliminate background noise. Particles were detected as regions where the pixel intensity fell above or below a particular threshold value. This enabled the separation of the dark (in focus) cells from the medium grey background and the white (out of focus) cells (Figure 11). After particle isolation, the script located the centroid (centre of mass) of each cell, using the function *regionprops* from the image processing toolbox in MATLAB. Cells could then be tracked from one frame to the next, following the X, Y position of the centroid, to produce movement trajectories. Tracks shorter than one second long were disregarded as they were considered too short to provide an accurate representation of the motility patterns.

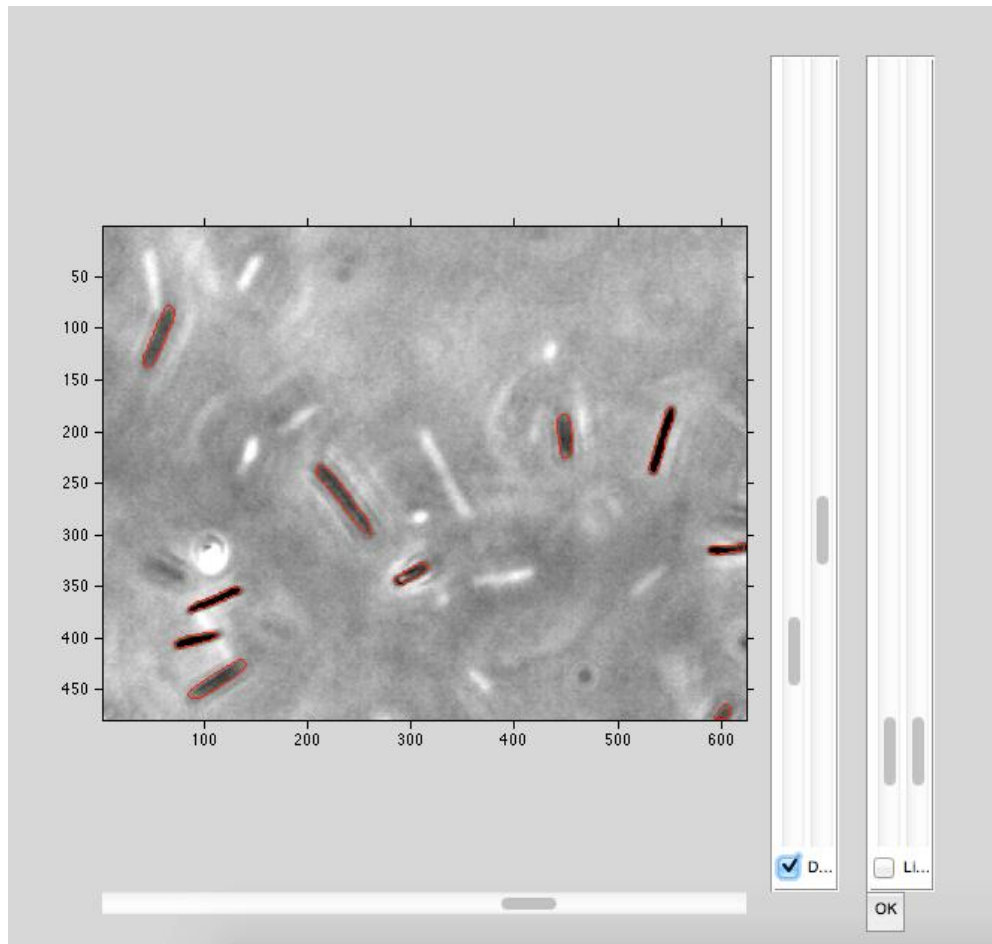


**Figure 11:** Matlab thresholding process, used to isolate cells for tracking and create a measure of cell shape properties.

At this stage of the analysis, a range of data could be extracted for each frame within the video, and for each cell within that frame. Firstly, the position of each cell; the X and Y co-ordinates of the centroid were established, for each cell within each video frame. Moreover, several geometric parameters could be determined for each cell (within each frame) (Figure 12). The length of the cell was generated by the application of the *bwmorph* MATLAB function (image processing toolbox), which thinned the detected cell to create a skeleton line through the centre of the cell body shape. The major axial length was calculated as the arc length of these skeleton lines, extended to meet the boundary of the cell. The width of the cell was calculated as the length of the line perpendicular to the skeleton line, passing through the centroid, and touching the

boundary wall at either end. Other extracted parameters included; the aspect ratio of the cell (length/width), the perimeter length of the cell (the length of the boundary of the cell), and the orientation (angle) of the cell between the x-axis and the major axis (skeleton line) of the cell (determined using the *regionprops* MATLAB function).

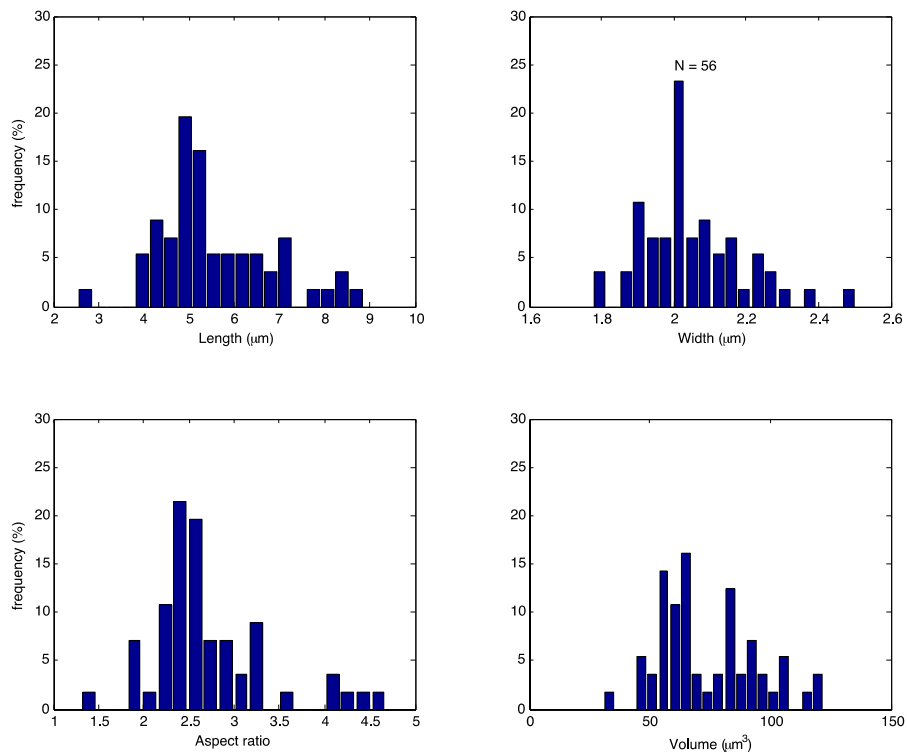


**Figure 12:** Cell size and shape statistics for each cell isolated within one two-minute video. Frequency histograms of longest axial length (μm) (top left), width – perpendicular to axial length (μm) (top right), aspect ratio (bottom left) and volume (bottom right) (μm<sup>3</sup>).

The ‘tracking’ part of the MATLAB code used the X and Y positions of the centroid, placing overlapping cells within the same track. This, combined with the orientation of the pole of the cell, was used to calculate the speed and rotational movement of each cell across each frame (Figure 13). From this, the length of each track and average speed across the length of the track could also be calculated.

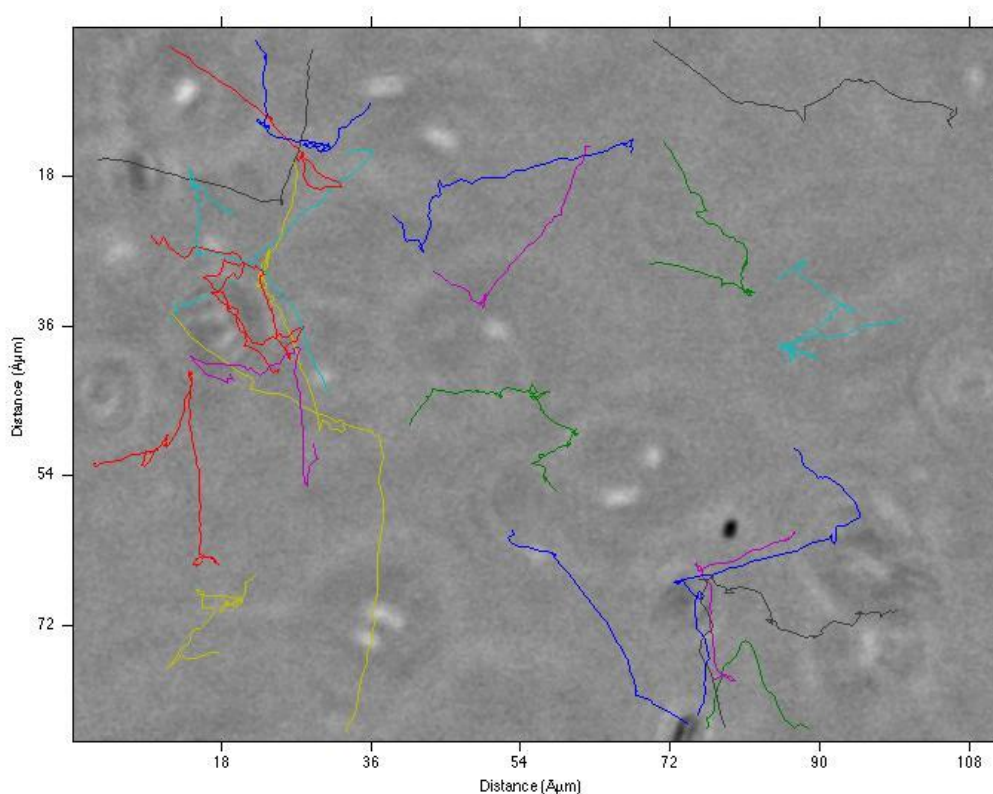


**Figure 4:** Visualization of all tracks recorded for an example two minute video (distance is in micrometres). (Colours are used to distinguish separate tracks and are not representative of any other characteristics).

### 2.2.6. Runs and Tumbles

Due to the nature of *E. coli* motility, it was necessary to separate the ‘runs’ and ‘tumbles’ within each recorded trajectory to gain a true representation of swimming behaviour. Each trajectory was re-analysed in MATLAB, with thresholding parameters set, to determine time periods displaying run and tumble behaviours (Figure 14). Tumbles

were considered to be any period where the cell speed dropped below  $4\mu\text{m/s}$ , or the change in orientation of the pole was greater than 10 degrees, across a moving average of 3 frames. Runs were considered longer than 10 frames (0.3 seconds), faster than the tumble speed and straighter than the tumble angle. Only complete runs were considered for analysis. Any recorded runs where the difference between the minimum and maximum recorded speeds was less than  $1\mu\text{m/s}$ , were considered to be passive cells drifting and were disregarded.

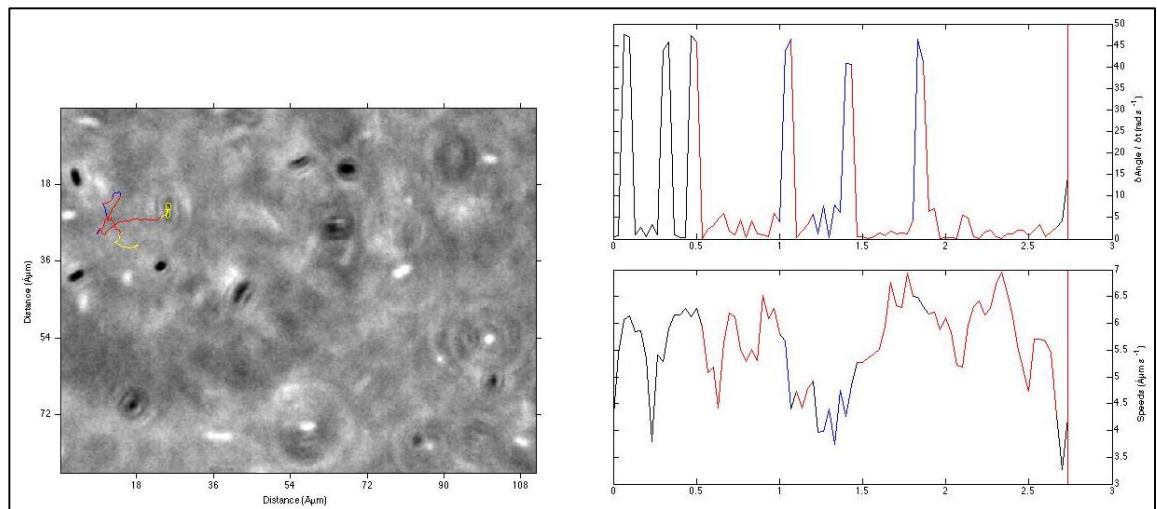


**Figure 14:** MATLAB plot displaying the thresholding process for runs and tumbles. Left: representation of runs and tumbles for a particular track (yellow: incomplete, so disregarded, Red: runs, Blue: tumbles). Right: (Red: runs, Blue: tumbles, Black: incomplete), Top-Right: Change in angle of the pole over time, Bottom-Right: Change in speed over time.

### 2.3. Data Analysis

Tracks from all videos were combined prior to analysis, to produce a single dataset consisting of 1498 cell tracks, with over 8000 runs, across a cell length range of 2 - 51  $\mu\text{m}$ . All data and figures used within the results were produced using R statistics software version; I386 3.0.2.INK (R Development Core Team 2009).

## 2.4. Results

Cells within a normal length range ( $3\mu\text{m} \pm 1\mu\text{m}$ ) were analysed to provide standard swimming statistics for cells of *E. coli* AW405 in minimal media (Figure 15). The mean run speed observed was  $14.49\mu\text{m/s}$  ( $n=215$ ,  $\sigma=7.2\mu\text{m/s}$ ), with each run lasting 0.29 seconds ( $n=215$ ) on average. Tumbles displayed a range of angles, with the most frequent observations occurring  $\pm 30$  degrees of the starting position. Tumble durations were shorter than runs, with a mean time of 0.25s ( $n=209$ ).

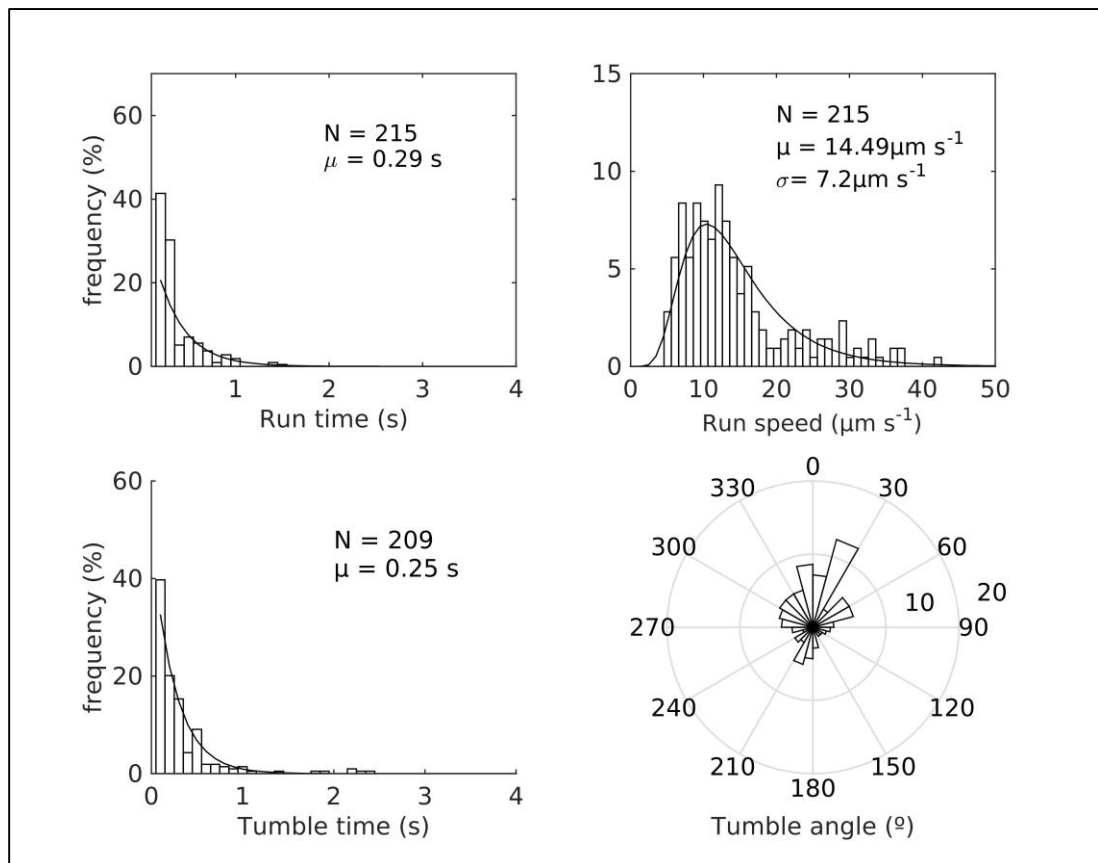


**Figure 15:** Track data from cells  $3\mu\text{m}$  long ( $\pm 1\mu\text{m}$ ), representing the normal length ranges of *E. coli* cells (Legends:  $n$ = number of individual data points,  $\mu$ =mean value,  $\sigma$ =variance). Top Left: observed run times (seconds); Top Right: observed run speeds (micrometres/second); Bottom Left: observed tumble times (seconds); Bottom Right: observed tumble angles (degrees).

Filamentous cells, within a length range ( $10\mu\text{m} \pm 1\mu\text{m}$ ) were analysed to provide a snapshot of filamentous swimming behaviours for cells of *E. coli* AW405 in minimal media (Figure 16). The mean run speed observed was  $15.13\mu\text{m/s}$  ( $n=654$ ,  $\sigma=8.47\mu\text{m/s}$ ), with each run lasting 0.46 seconds ( $n=654$ ) on average. Tumbles rarely occurred outside  $\pm 30$  degrees of the starting position. Tumble durations were shorter than runs, with a mean time of 0.13s ( $n=625$ ).

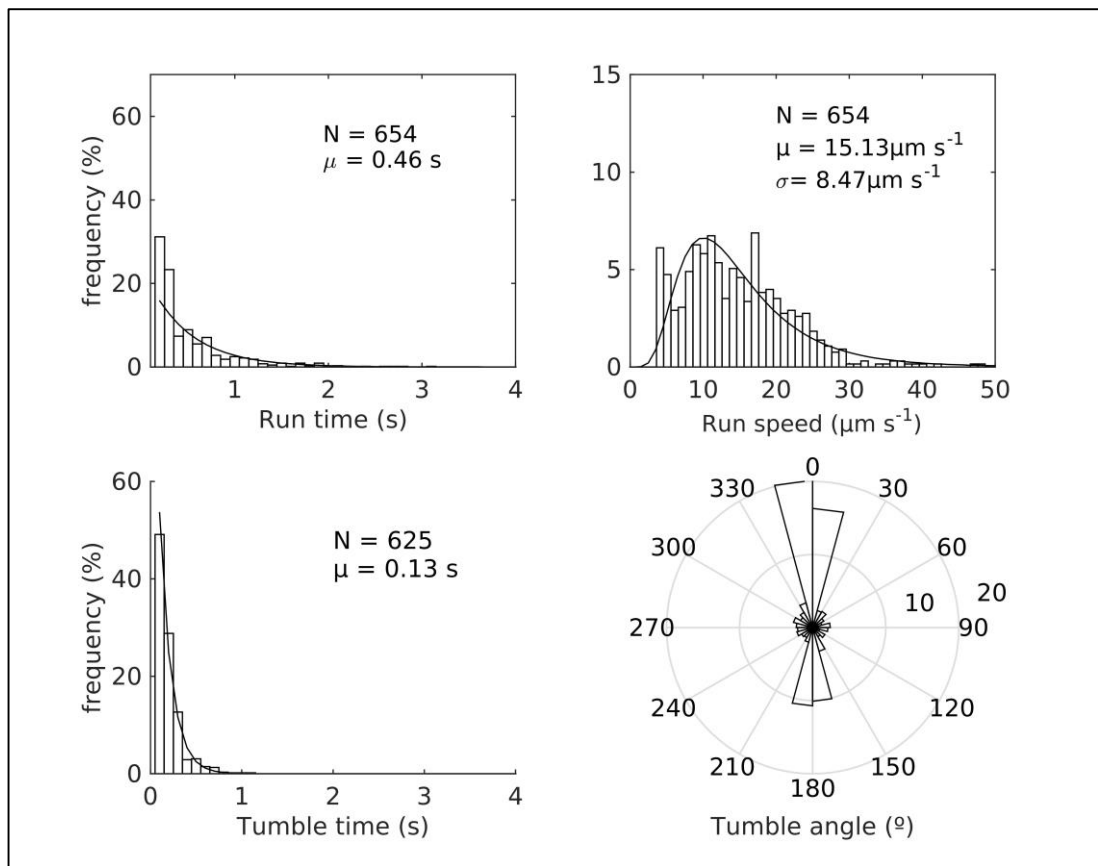


**Figure 16:** Track data from filamentous *E. coli* cells  $10\mu\text{m}$  long ( $\pm 1\mu\text{m}$ ), (Legends:  $n$ = number of individual data points,  $\mu$ =mean value,  $\sigma$ =variance). Top Left: observed run times (seconds); Top Right: observed run speeds (micrometres/second); Bottom Left: observed tumble times (seconds); Bottom Right: observed tumble angles (degrees).

A range of cell sizes were observed throughout the tracking experiments, from  $2\mu\text{m}$  to  $51\mu\text{m}$  long in the major axial dimension, with the number of observations decreased with an increase in size (Figure 18). Similarly, when considering the cell body aspect ratios observed within experiments, the frequency of observed aspect ratios also decreases with increasing cell elongation (Figure 19).

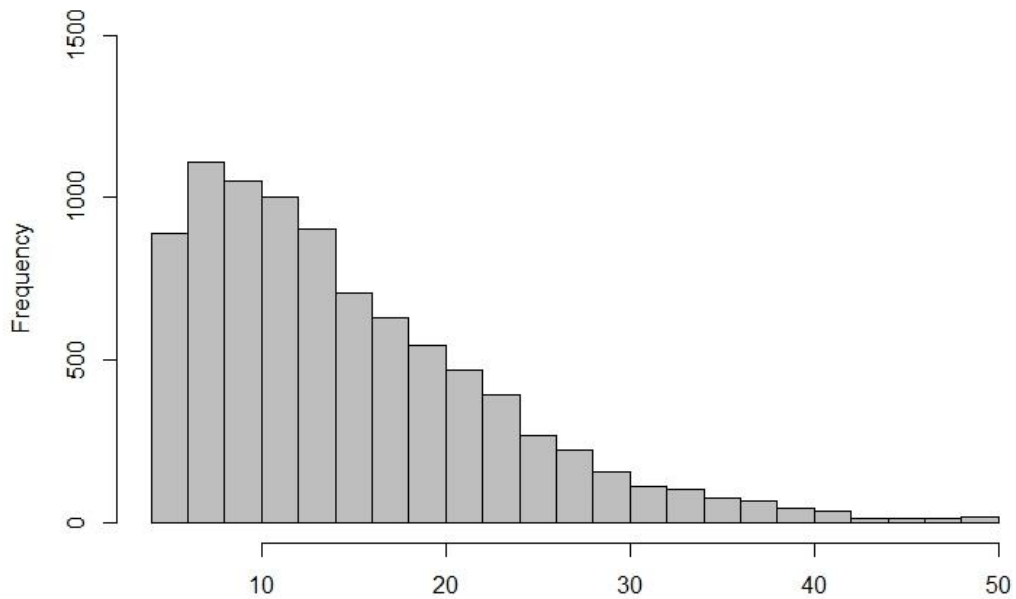


**Figure 5:** Frequency of mean cell lengths observed for each ‘run’ analysed.

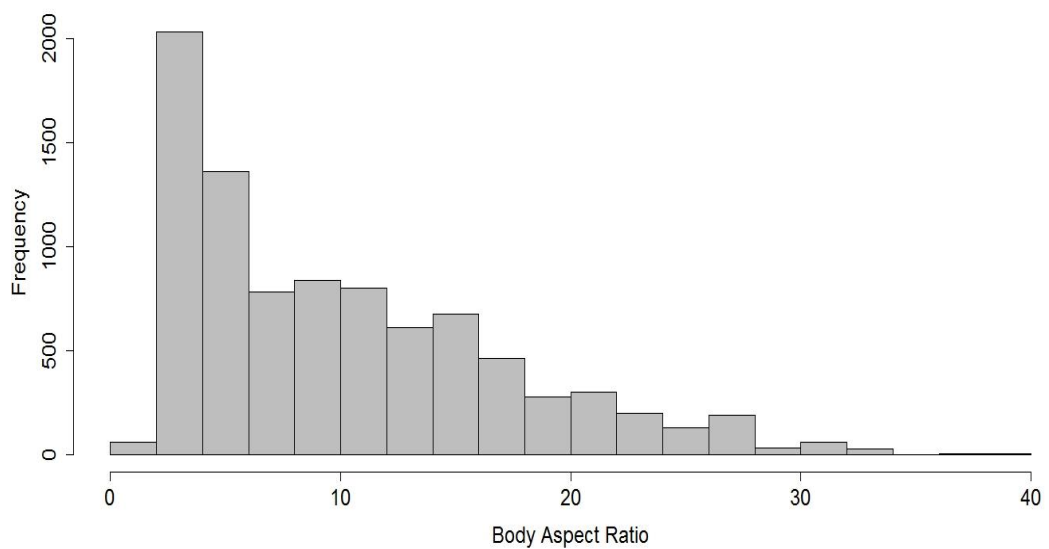


**Figure 68:** Frequency of body aspect ratios (length/width) observed for each ‘run’ analysed.

Linear model regression analysis was employed to further understand the trajectory data.

A simple linear model regression was calculated to predict the changes in run speed, based upon increasing in cell length (Figure 20). A significant regression equation was found ( $F_{1, 8858} = 130.5$ ;  $P < 0.001$ ), with an adjusted  $R^2$  value of 0.0144. Run speed decreased approximately -0.109 micrometres per second for each micrometre increase in cell length.

A simple linear model regression was also calculated to predict the changes in tumble lengths, based upon increasing in cell length (Figure 21). A significant regression equation was found ( $F_{1, 8265} = 11.22$ ;  $P < 0.001$ ), with an adjusted  $R^2$  value of 0.001. The amount of time spent tumbling decreased approximately -0.001 seconds for each micrometre increase in cell length. The length of tumble events were very slightly negatively correlated with increasing cell axial lengths (Figure 21), signifying that larger/more elongate cells tumble for incrementally smaller periods of time than shorter cells.

A simple linear model regression was calculated to predict the changes in swimming speed (body lengths per second), based upon increasing in cell length (Figure 22). A significant regression equation was found ( $F_{1, 8858} = 18160$ ;  $P < 0.001$ ), with an adjusted  $R^2$  value of 0.6721. The run speed (body lengths per second) decreased approximately -1.0959 seconds for each micrometre increase in cellular length.

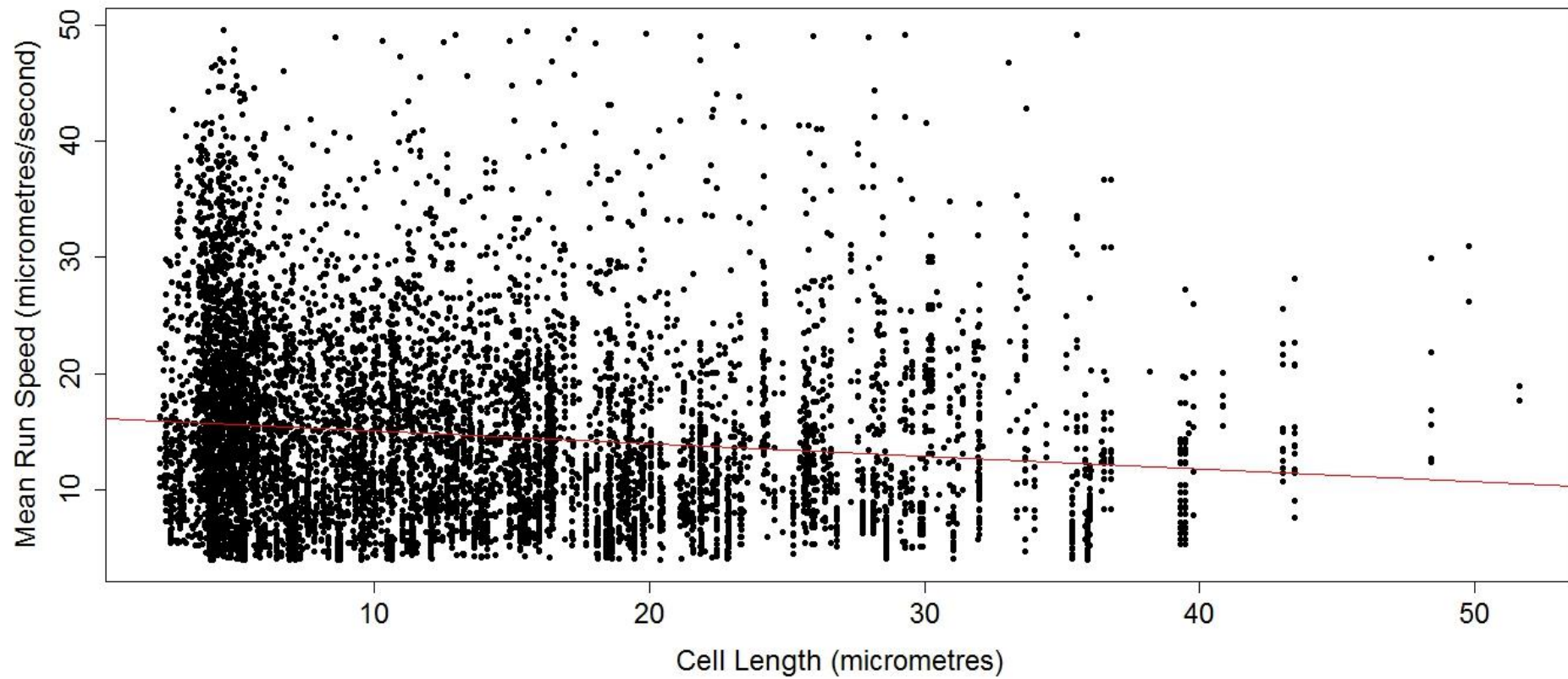


**Figure 19:** Negative correlation observed between the major axial length (micrometres) of the cell and its mean run speed (micrometres per second). Red line denotes the linear regression model

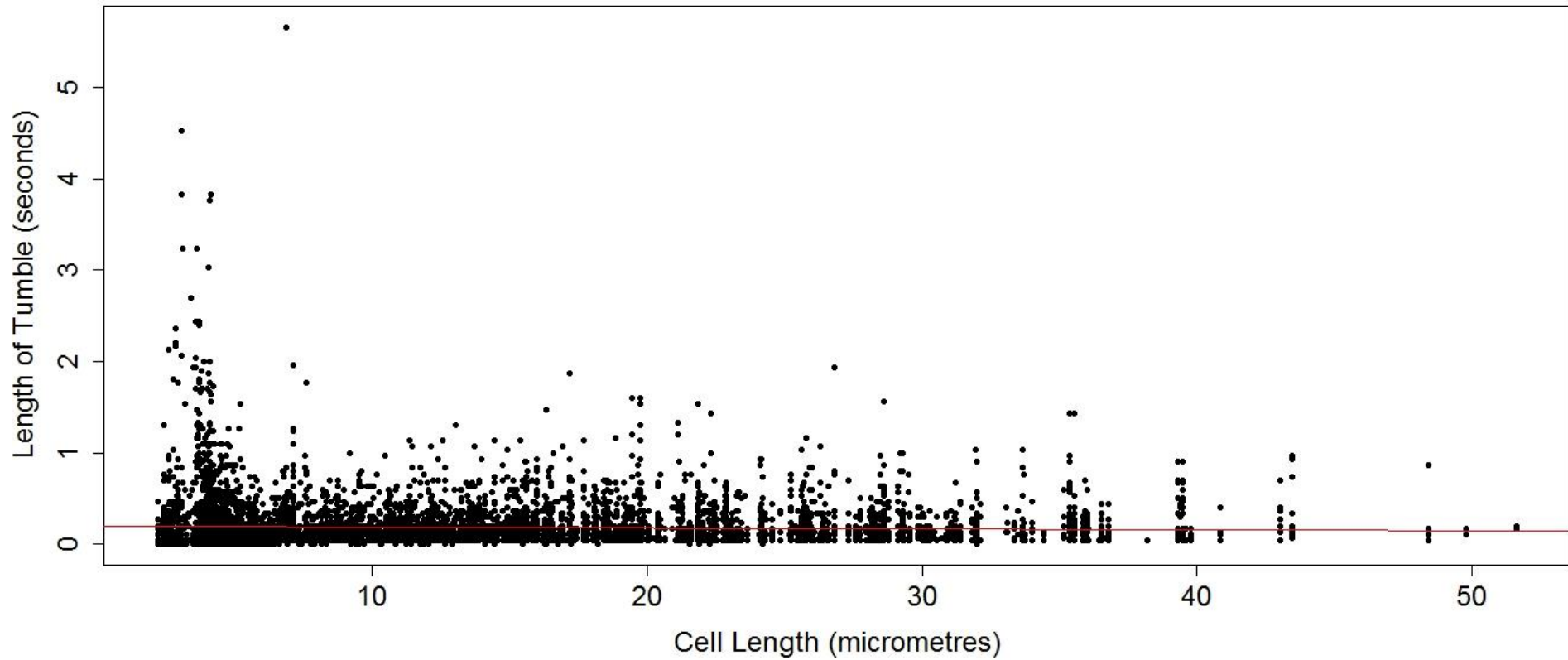


**Figure 20:** Observed variations in tumbling events (seconds) are very slightly negatively correlated with increases in cell length (micrometres) Red line denotes the linear regression model.

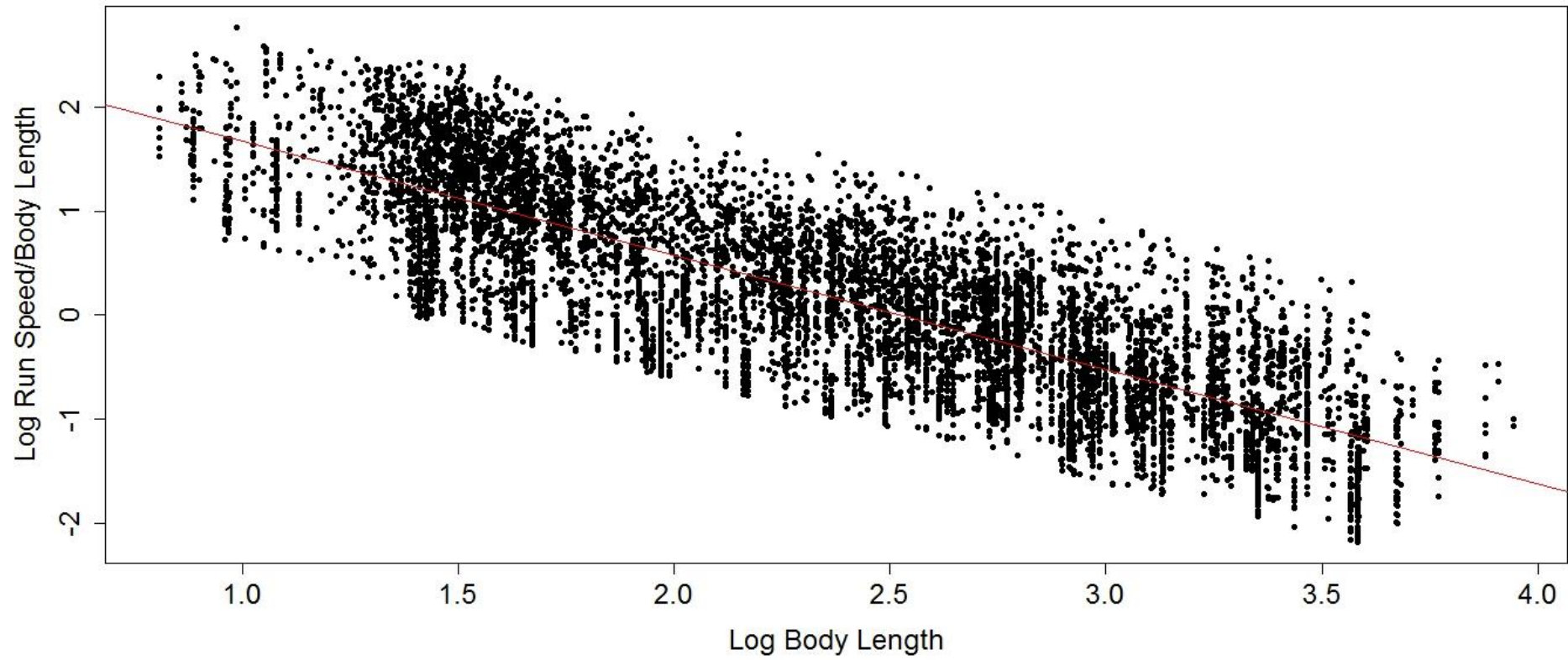


**Figure 21:** The change in run speeds as a measure of log body lengths per second (length specific swimming speed) with increasing cell body sizes. Red line denotes the linear regression model.

## 2.5. Discussion of Results

There was a natural decrease in the number of cells observed with increasing cell size (Figure 13). This was primarily due to the protocol used for these experiments; with the addition of cephalixin all cell division is rapidly halted. However, cell size increases led to an increase in the overall cell density of the culture, without an increase in the number of cells. Consequently, for larger cell sizes, dilutions had to be carried out for optimal viewing, and thus fewer cells remained within the sample for observation. To gain a clearer representation of larger filamentous cells, more replicates would need to be undertaken at the larger size ranges (approximately >4 hours after antibiotic inoculation).

Similarly, cell aspect ratios also followed this trend (Figure 14), with fewer observations recorded from cells that were elongated. This highlights that cell width remained fairly constant throughout all of the experiments, as would be expected with this type of treatment.

Initial comparisons were made between normal sized cells of  $3\mu\text{m}$  ( $\pm 1\mu\text{m}$ ) and elongated cells of  $10\mu\text{m}$  ( $\pm 1\mu\text{m}$ ) (Figures 15 & 16 respectively), showed that filamentous cells had a tendency to run and reverse rather than run and tumble (this was confirmed with visual observations). The changes in angles of orientation observed during ‘tumbling events’ were much smaller in the filamentous cells. This suggests that once cells reach a certain size ( $>10$  micrometres in length), the directional change in flagella rotation is unable to generate enough force to turn the cell body towards a new direction. Consequently, the cell reverses moving backwards for a short period of time, before continuing on its original path.

Normal sized cells were observed to move at a rate similar to those first observed by Berg and Brown (1972) at approximately 14 micrometres per second (mean=14.49  $\mu\text{m/s}$ ) during the 'run' phase (Figure 15). Whereas elongated cells (10 $\mu\text{m}$  (+/-1 $\mu\text{m}$ )), moved slightly faster, at a mean speed of 15.13  $\mu\text{m/s}$  (Figure 16). Furthermore, longer cells spent more time running, and less time tumbling than normal sized cells (Figures 15, 16 & 21). This could be attributed to the larger cells being unable to tumble efficiently, and adopting a 'run and reverse' behavioural mechanism instead of the traditional 'run and tumble'.

When considering the dataset as a whole, longer cells were observed to 'run' (straight-line swimming) more slowly than their smaller counterparts. This could be attributed to a lack of synchronicity in the rotation of the flagella, due to the development of multiple flagella bundles along the length of the cell, suggested by Maki *et al.*, (2000). Furthermore, the short-range nature of the chemotactic signalling pathway (Ishihara *et al.*, 1983) could further hinder the synchronous movements of the individual filaments, as some of the flagella motor may be too far away from the large sensory complexes located at the pole of the cell (Sourjik, 2004). Although it has been suggested that filamentous cells generate chemoreceptors along the length of their body (Maki *et al.*, 2000), it currently remains unclear whether these chemoreceptors are fully functional, and how the introduction of multiple chemical detection sites affects the synchronicity of the flagella motors. Moreover, increased elongation of the cell body and the addition of more flagella would also lead to an increase viscous drag, further slowing the movement of the cells (Dusenbury, 2009). Due to observations at 10 $\mu\text{m}$  (+/-1 $\mu\text{m}$ ) indicating a higher swimming rate, it could be suggested the cells speed up slightly

with small changes in axial length, but slow down after a threshold length is reached. Further experiments would need to be undertaken to investigate this hypothesis, and to pinpoint exact threshold values for these occurrences.

By plotting a linear regression of the changes in length specific run speed with changes in body length (Figure 22), similarities can be observed between our data and the existing literature (see Figure 2 from Vogel). The data follows the same general trend of reduced length specific cell speed at increasing cell lengths. However, due to the small sample of species currently examined, any definitions of allometric scaling trends between body size and swimming speed for microorganisms would be inadequate at this time. With an increase in research directed towards swimming microorganisms, and rapid advances in imaging techniques, this remains a future goal.

Overall, this study found that there were significant effects on the natural motile behaviours of *E. coli* cells with increasing cell lengths. Alterations in motility with response to changes in cell axial length clearly show that cell shape must play an important role in the swimming of microorganisms. The understanding of microbial shape to date is very limited, and further exploration into the evolution of the range of forms observed in nature, is key to developing a greater understanding of life at low Reynolds numbers.

### 2.5.1 Personal Observations

Within experiments, elongated cells were observed to run and reverse rather than reorienting via tumbling. Furthermore, over the course of the experimentation period cells of larger axial lengths were observed to ‘wobble’, both at the poles of the cell, and along its axis. As a result of the rigidity properties of the MreB protein contained in the longitudinal axis of the cell, this observation can be attributed to the natural rotational movement of the cell body coupled with the slightly curved rod shapes which arise through filamentation. It would be possible to confirm this through the application of holographic microscopy, to gain 3D renderings of the swimming cells. Furthermore, by dyeing the flagella of these elongated forms, the positions of flagella bundles, and the rotation behaviours could be observed.

### 2.6. Conclusions

The aim of this experiment was to explore the effects of changes in the axial length of a cell on expressed motile behaviours. Specific focus was placed upon the known run and tumble behavioural responses of *Escherichia coli*. Key areas of interest were; a) the run speed of the cell, b) the angle of tumbling, c) the duration of both runs and tumbles, and d) any unexpected observations.

This experiment has demonstrated that changes in the axial length of a cell have an effect on the motile behaviours of *E. coli* cells. Filamentous cells of *E. coli* were observed to run and reverse, rather than run and tumble. This could be attributed to a significant decrease in the angle of rotation during tumbling events, within elongated cells. Increased cell size led to an initial increase in the run speed, however, this

declined significantly at the larger size ranges. Furthermore, the duration of tumble events also decreased slightly with increasing cell lengths, however there was no significant difference observed in the duration of run periods. Overall these results, coupled with personal observations, suggest that larger filamentous cells of *E. coli* face a reduction in overall speed and ability to randomly re-orientate their directionality.

This study has highlighted the importance of specific body shapes to the swimming mechanisms of motile microorganisms. It is possible that only slight changes in the axial lengths of cells could modify motile behaviours, making them more/less effective. Exploration of inter- and intra- species variations in swimming behaviours is needed to truly understand the function of specific shapes to the life of bacterial cells. It is hoped that further exploration of shape changes within a single species can reveal at least some of the ecological pressures that have led to the evolution of such a diverse array of organism shapes within the microbial world.

**Chapter 3:**  
**General Discussion**

## **3.0 General Discussion**

### **3.1.1 3D Tracking**

One of the key limitations of the techniques used within these experiments; is the inability to film cells within the Z direction. Restricting cells to a thin film, only a few micrometres in depth may have significant effects on the natural motility behaviours of *E. coli* cells. Conventional light microscopy (including phase contrast and differential interference contrast) is only capable of capturing images directly on the focal plane, making data acquisition in the Z direction very limited. Due to the rapid nature of swimming cells, scanning microscopes are often too slow to capture necessary rapid behavioural responses expressed by living cells. Howard Berg's 3D tracking microscope developed in the 1970s is able to 'lock on' to a single micro-organism (in this case *E. coli*) and follow it in three-dimensions, enabling observations of vertical movement for a single cell (Berg & Brown, 1972). However, the main drawback of this technique is its inability to study multiple organisms simultaneously, consequently resulting in very small sample sizes and larger replications. In comparison, digital holography is an emerging technique that has the capacity to track the positions of multiple cells simultaneously in three dimensions (Figure 18) (Molaei *et al.*, 2014; Giuliano *et al.*, 2014). However, this system is computationally expensive, as it requires the application of mathematical algorithms (either Lorenz-Mei theory (Lee *et al.*, 2007) or Rayleigh–Sommerfeld Back propagation (Lee & Grier, 2007)) to reconstruct the holographic data.

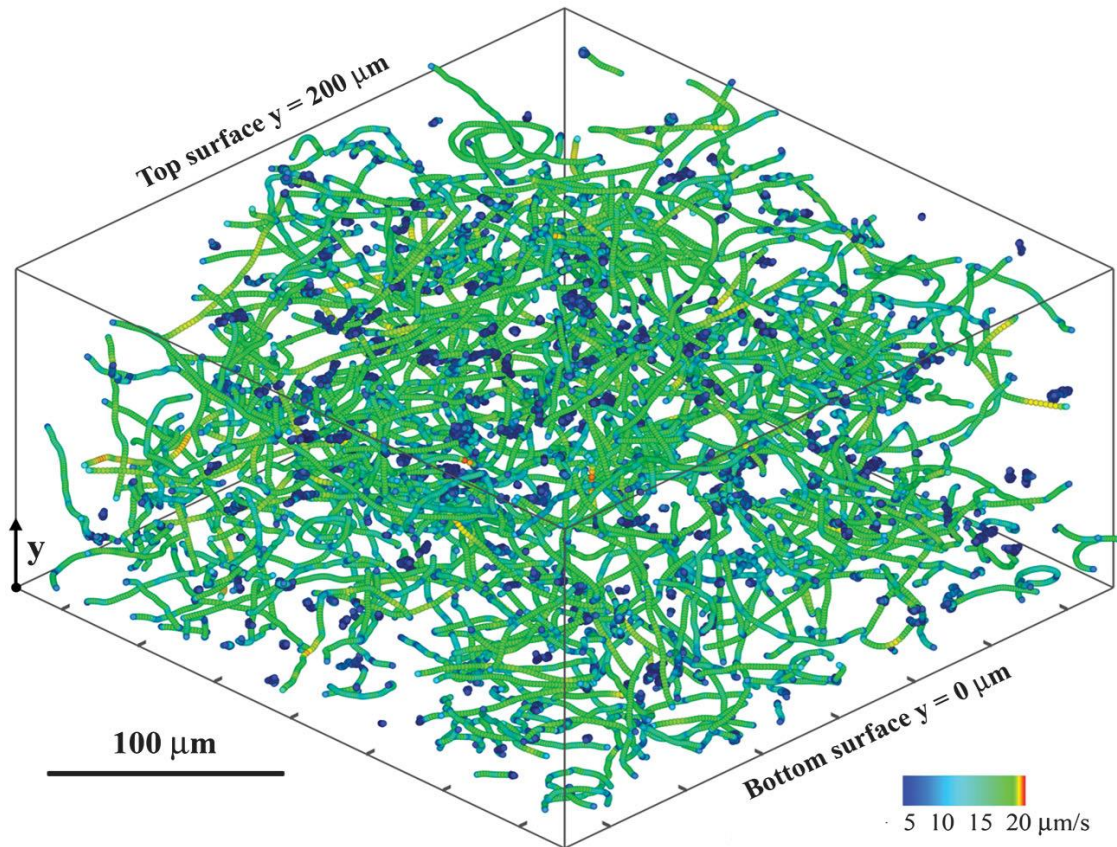


**Figure 7:** Trajectories of multiple *E. coli* cells tracked using digital holography (Molaei *et al.*, 2014).

### 3.1.2 Wall Effects

For organisms living at low Reynolds numbers, movement can be significantly affected by ‘wall effects’. The presence of an object, in this case the confinements of a microscope slide, can alter the fluid flow patterns surrounding the cell. Close proximity to walls at low Reynolds numbers can significantly add to the drag of swimming microorganisms (Winet, 1993). It has been suggested that when cells of *E. coli* move with 20μm of a solid surface, tumbles may be suppressed by up to 50% (Molaei *et al.* 2014). A guide that is often used within biological experiments for testing whether or not the wall effects acting upon swimming microorganisms can be ignored is; equation 2.

## Equation 2

$$\frac{y}{l} > \frac{20}{Re}$$

Whereby  $y$  is the distance to the nearest solid wall,  $l$  is the characteristic length of the object (usually the longitudinal axis), and  $Re$  is the Reynolds number (Vogel, 1994).

## 3.2. Outstanding Questions

### 3.2.1. What Effect does Filamentation Have on Chemotactic Responses?

Microorganisms use chemical receptors (chemoreceptors) located within their cell membrane to locate areas of higher nutrient concentrations, and move away from areas which may be detrimental to their growth and development. These receptors are highly specific, allowing the detection of only a small number of chemicals. *E. coli* are thought to have a minimum of 3 types of chemoreceptor specific to the amino acids; serine, galactose and aspartate (Hazelbauer & Adler, 1971; Mesibov & Adler, 1972). The serine receptor shows a strong response towards serine, and a weaker response to cysteine, alanine, glycine and l-glutamate. The galactose receptor responds to galactose and glucose, and the aspartate receptor is thought to only be responsive to aspartate itself (Hazelbauer *et al.*, 1969; Brown & Berg, 1973). Studies have shown that in the presence of each of the above chemical cues, cells migrate towards areas with higher concentrations of stimulus, through the

suppression of the 'tumble' behavioural response (Adler, 1973; Berg & Brown, 1972; Brown & Berg, 1973). *E. coli* cells are able to bias the 'random walk movement', in the presence of an attractant, by reducing the frequency of their tumble movements, creating a greater accuracy in the direction of travel towards the positive stimuli and an increase in the average cell velocity. Increases in cell velocity are thought to be the central behavioural response used in chemotaxis to provide the largest increase the rate of nutrients encountered by motile cells (Blackburn & Fenchel, 1999). Similarly, when a cell encounters a deterrent stimulus, the frequency of tumbles increases in an attempt to direct the cell away from negative environments (Macnab & Koshland, 1972).

Chemoreceptors located in the cell membrane form clusters at the poles of the cell alongside several protein receptors (including; MCP the methyl-accepting chemotaxis protein, and both CheA and CheW intracellular proteins). These large sensory complexes transmit signals from the chemoreceptors to the flagella motors, via a series of phosphorylation events along the trans-membrane reception pathway (Maddox & Shapiro, 1993; Sourjik, 2004). When a stimulus is detected by the cell, a hyperpolarizing wave sent from the sensory complex moves along the membrane and is received by the flagella motors (Szmelcman & Adler, 1976). This short-range signal (a maximum of 10 $\mu$ m long from the source of the stimulus) enables the activation or suppression of changes in the rotational movement of the flagella; thus allowing the cell to re-orientate itself towards the most desirable location (Segall *et al.*, 1984). The detection and transmission process is thought to take approximately one second, similar to the duration of an average 'run', as longer time-frames would have a negative impact on a cell's ability to bias the 'Random Walk'; and durations longer than five seconds would prevent the process entirely (Berg & Purcell, 1977).

Due to the nature of the signal in normal *E. coli* cells being short-range, and the specific location of the chemoreceptors at the poles of the cell, I propose to investigate the changes in chemotaxis behaviours within filamentous cells of *E. coli*, forming a range of aspect ratios. Specific questions to be tackled along this topic include:

- Would the cells synthesize chemoreceptors along the length of the cell?
- Would the cell reach a length at which chemotaxis no-longer occurred?
- Are these changes in behavioural response applicable to all three types of chemoreceptor?
- Due to the reduction in tumbling associated with increased axial length, would filamentous cells be able to reach nutrient patches more rapidly than untreated cells?

### 3.2.2. How do Changes in Cell Shape Affect Motility? The Study of Spherical *E. coli* and other Shapes compared with Filamentous and Untreated Forms.

Bacterial cells naturally occur in a vast number of different shapes, the most common of which are the rod and coccoid forms. Changes in cell morphology are usually linked with environmental pressures these include; predation, nutrient uptake, and motility (Young, 2007). However, the question; why does that particular bacterium have that specific shape, remains largely unanswered.

In many bacterial cells, the MreB protein has been linked to both rod and more complex shapes (ellipsoidal, helical & filamentous), however is absent in both gram-positive and gram-negative spherical cells. Consequently, it has been suggested that coccoid cells are the default prokaryotic shape, which occurs in the absence of these structural proteins (Jones *et al.*, 2001). A22 (*S*-benzylisothiurea) is a recently discovered compound that can be used to induce coccoid cell shapes within rod-shaped and more complex prokaryotic cells (Iwai *et al.*, 2002). When added to bacterial cultures, A22 binds to specific ATP sites, significantly reducing the availability of ATP, thus preventing the synthesis of the rigid filaments that provide structure to bacterial cell walls (Bean *et al.*, 2009). At concentrations of 10 µg/ml and below, the addition of A22 results in an increase in cell 'roundedness' until the point of entirely spherical cells, occurring a few hours after treatment. However, when added at concentrations of 100µg/ml and above, cell growth appears to be completely halted, but cell shape is not affected (Gitai *et al.*, 2005). Moreover, the inhibition of MreB through the addition of A22 appears to have no other effects on cell functioning, including DNA segregation and other cell division processes (Karczmarek, 2007). Consequently, when A22 is added to bacterial cells (including *E. coli*), those cells develop less structured cell walls and become coccoid in shape, without any other known physiological effects taking place.

By combining the A22 with the antibiotic used in this study (cephalexin), it is possible to generate spherical cells of a range of sizes, which physiologically behave the same as untreated cells, except for their inability to divide. If these cells are grown in shaped chambers, similar to jelly moulds, but at the micrometre scale, they will adopt the chamber shape, and a range of cell morphologies could be produced (Takeuchi, *et al.*, 2005). This would enable an array of questions based on the

importance of size and shape in motile microorganisms, to be tackled. Including (but not limited to):

- What is the optimal size/shape for swimming?
- How does this change with changing environments?
- How do changes in size and shape affect chemotactic responses?
- What is the preferential size/shape targeted by a predator for a prey item?

## References

- Adler, J., (1973) A Method for Measuring Chemotaxis and Use of the Method to Determine Optimum Conditions for Chemotaxis by *Escherichia coli*. *Journal of General Microbiology*. **74**: 77–91.
- Adler, J., & Templeton, B., (1967) The Effect of Environmental Conditions on the Motility of *Escherichia coli*. *Journal of General Microbiology*. **46**: 175–184.
- Armstrong, J.B., Adler, J., & Dahl, M., (1967) Non-chemotactic Mutants of *Escherichia coli*. *Journal of Bacteriology*. **93**: 390–398.
- Bardy, S.L., Ng, S.Y.M., & Jarrell, K.F., (2003) Prokaryotic Motility Structures. *Microbiology*. **149**: 295–304.
- Bean, G.J., Flickinger, S.T., Westler, W.M., McCully, M.E., Sept, D., Weibel, D.B., & Amann, K.J., (2009) A22 Disrupts the Bacterial Actin Cytoskeleton by Directly Binding and Inducing a Low-Affinity State in MreB. *Biochemistry*. **48**: 4852–4857.
- Berg, H.C., (1983) Random Walks in Biology. *Princeton University Press*. Expanded edition. p.5-6.
- Berg, H.C., (1996) Symmetries in Bacterial Motility. *Proceedings of the National Academy of Sciences*. **93**: 14225–14228.
- Berg, H.C., (2000) Motile Behaviour of Bacteria. *Physics Today*. **53**: 24–29.

- Berg, H.C., (2003) The Rotary Motor of Bacterial Flagella. *Annual Review of Biochemistry*. **72**: 19–54.
- Berg, H.C., (2004) *E. coli* in Motion. *Springer*. p.31-32, p.49-50.
- Berg, H.C., & Brown, D.A., (1972) Chemotaxis in *Escherichia coli* Analysed by Three-Dimensional Tracking. *Nature*. **239**: 500–505.
- Berg, H.C., & Purcell, E.M., (1977) Physics of Chemoreception. *Biophysical Journal*. **20**: 193.
- Berg, H C, & Turner, L, (1979) Movement of Microorganisms in Viscous Environments. *Nature*. **278**: 349-351.
- Blackburn, N., & Fenchel, T., (1999) Influence of Bacteria Diffusion and Shear on Micro-scale Nutrient Patches and Implications for Bacterial Chemotaxis. *Marine Ecology Progress Series*. **189**: 1–7.
- Brennen, C., & Winet, H., (1977) Fluid Mechanics of Propulsion by Cilia and Flagella. *Annual Review of Fluid Mechanics*. **9**: 339–398.
- Brown, D.A., & Berg, H.C., (1974) Temporal Stimulation of Chemotaxis in *Escherichia coli*. *Proceedings of the National Academy of Sciences*. **71**: 1388–1392.
- Brown, J.H., & West, G.B., (2000) Scaling in Biology. *Oxford University Press*. pp. 2-4 & 231-233.

- Codling, E.A., Plank, M.J., & Benhamou, S., (2008) Random Walk Models in Biology. *Journal of the Royal Society Interface*. **5**: 813–834.
- Cooper, S., & Denny, M.W., (1997) A Conjecture on the Relationship of Bacterial Shape to Motility in Rod-Shaped Bacteria. *Microbiology Letters*. **148**: 227–231.
- Crawford, D.W., (1992) Metabolic Cost of Motility in Planktonic Protists: Theoretical Considerations on Size Scaling and Swimming Speed. *Microbial Ecology*. **24**: 1–10.
- Darnton, N.C., Turner, L., Rojevsky, S., & Berg, H.C., (2006) On Torque and Tumbling in Swimming *Escherichia coli*. *Journal of Bacteriology*. **189**: 1756–1764.
- Denny, M.W., (1993) Air and Water; The Biology and Physics of Life's Media. *Princeton University Press*. p.58-67.
- Doi, M., Wachi, M., Ishino, F., Tomioka, S., Ito, M., Sakagami, Y., Suzuki, A., & Matsubishi, M., (1988) Determinations of the DNA Sequence of the MreB Gene and of the Gene Products of the Mre Region that Function in Formation of the Rod Shape of *Escherichia coli* Cells. *Journal of Bacteriology*. **170**: 4619–4624.
- Doolittle, R.F., & York, A.L., (2002) Bacterial Actins? An Evolutionary Perspective. *BioEssays*. **24**: 293–296.
- Dusenbery, D.B., (1997) Minimum Size Limit for Useful Locomotion by Free-Swimming Microbes. *Proceedings of the National Academy of Sciences*. **94**: 10949–10954.

- Dusenbery, D.B., (1998) Fitness Landscapes for Effects of Shape on Chemotaxis and Other Behaviours of Bacteria. *Journal of Bacteriology*. **180**: 5978–5983.
- Dusenbury, D.B., (2009) Living at Micro Scale – The Unexpected Physics of Being Small. *Harvard University Press*. p.23-25.
- Fletcher, D.A., & Mullins, R.D., (2010) Cell Mechanics and the Cytoskeleton. *Nature*. **463**: 485-492
- Flores, H., Lobaton, E., Mendez-Diez, S., Tlupova, S., & Cortez, R., (2005) A Study of Bacterial Flagella Bundling. *Bulletin of Mathematical Biology*. **67**(1): 137-168.
- Gitai, Z., Dye, N.A., Reisenauer, A., Wachi, M., & Shapiro, L., (2005) MreB Actin-Mediated Segregation of a Specific Region of a Bacterial Chromosome. *Cell*. **120**: 329–341.
- Giuliano, C.B., Zhang, R., & Wilson, L.G., (2014) Digital Inline Holographic Microscopy (DIHM) of Weakly-scattering Subjects. *Journal of Visualised experiments*. **84**, e50488.
- Goodell, E.W., Lopez, R., & Tomasz, A., (1976) Suppression of Lytic Effect of Beta Lactams on *Escherichia coli* and Other Bacteria. *Proceedings of the National Academy of Sciences*. **73**: 3293–3297.
- Greenwood, D., & O’Grady, F., (1973a) The Two Sites of Penicillin Action in *Escherichia coli*. *Journal of Infectious Diseases*. **128**: 791–794.

- Greenwood, D., & O'Grady, F., (1973b) Comparison of the Responses of *Escherichia coli* and *Proteus mirabilis* to Seven  $\beta$ -lactam Antibiotics. *Journal of Infectious Diseases*. **128**: 211–222.
- Guadayol-Roig, O., Thornton, K.L., & Humphries, S., (2014) Role of Bacterial Shape on Swimming Directionality. (*In preparation*).
- Guasto, J.S., Rusconi, R., & Stocker, R., (2012) Fluid Mechanics of Microorganisms. *Annual Review of Fluid Mechanics*. **44**: 373-400.
- Hazelbauer, G.L., & Adler, J., (1971) Role of the Galactose Binding Protein in Chemotaxis of *Escherichia coli* Toward Galactose. *Nature*. **230**: 101–105.
- Hazelbauer, G.L., Mesibov, R.E., & Adler, J., (1969) *Escherichia coli* Mutants' Defective in Chemotaxis Toward Specific Chemicals. *Proceedings of the National Academy of Sciences*. **64**: 1300–1307.
- Ishihara, A., Segall, J.E., Block, S.M., & Berg, H.C., (1983) Coordination of Flagella on Filamentous Cells of *Escherichia coli*. *Journal of Bacteriology*. **155**: 228–237.
- Iwai, N., Nagai, K., & Wachi, M., (2002) Novel S-Benzylisothiourea Compound that Induces Spherical Cells in *Escherichia coli*, Probably by Acting on a Rod-shape-determining Protein(s) Other than Penicillin-binding Protein 2. *Bioscience, Biotechnology and Biochemistry*. **66**: 2658–2662.
- Jarrell, K. F., & McBride, M.J., (2008) the Surprisingly Diverse Ways that Prokaryotes Move. *Nature Reviews Microbiology*. **6**: 466-476.

- Johansen, J.E., Pinhassi, J., Blackburn, N., Zweifel, U.L., & Hagstrom, A., (2002) Variability in Motility Characteristics Among Marine Bacteria. *Aquatic Microbial Ecology*. **28**: 229–237.
- Jones, L.J., Carballido-López, R., & Errington, J., (2001) Control of Cell Shape in Bacteria: Helical, Actin-like Filaments in *Bacillus subtilis*. *Cell*. **104**: 913–922.
- Juarez, J.R., & Margolin, W., (2012) A Bacterial Actin Unites to Divide Bacterial Cells. *The EMBO Journal*. **31**: 2235–2236.
- Kac, M., (1947) Random Walk and the Theory of Brownian Motion. *The American Mathematical Monthly*. **54**: 369.
- Karczmarek, A., Baselga, R.M.-A., Alexeeva, S., Hansen, F.G., Vicente, M., Nanninga, N., & den Blaauwen, T., (2007) DNA and Origin Region Segregation are not Affected by the Transition from Rod to Sphere after Inhibition of *Escherichia coli* MreB by A22. *Molecular Microbiology*. **65**: 51–63.
- Kareiva, P.M., & Shigesada, N., (1983) Analyzing Insect Movement as a Correlated Random Walk. *Oecologia*. **56**: 234–238.
- Koch, A.L., (1996) What Size Should a Bacterium Be? A Question of Scale. *Annual Reviews in Microbiology*. **50**: 317–348.
- Kudo, S., Magariyama, Y., & Aizawa, S.-I., (1990) Abrupt Changes in Flagellar Rotation Observed by Laser Dark-Field Microscopy. *Nature*. **346**: 677–680.

- Lee, S.H., Roichman, Y., Yi, G.R., Kim, S.H., Yang, S.M., Blaaderen, A., Oostrum, P., & Grier, D.G., (2006) Characterising and Tracking Single Colloidal Particles with Video Holographic Microscopy. *Optics Express*. **15**(26): 18275-18282.
- Lee, S.H., & Grier, D.G., (2007) Holographic Microscopy of Holographically Trapped Three-Dimensional Structures. *Optics Express*. **15**(4): 1505-1512.
- Lighthill, M.J., (1969) Hydromechanics of Aquatic Animal Propulsion. *Annual Review of Fluid Mechanics*. **1**: 413–446.
- Lowe, G., Meister, M., & Berg, H.C., (1987) Rapid Rotation of Flagellar Bundles in Swimming Bacteria. *Nature*. **325**: 637–640.
- Macnab, R.M., (1977) Bacterial Flagella Rotating in Bundles: a Study in Helical Geometry. *Proceedings of the National Academy of Sciences*. **74**: 221–225.
- Macnab, R.M., & Koshland, D.E., (1972) The Gradient-sensing Mechanism in Bacterial Chemotaxis. *Proceedings of the National Academy of Sciences*. **69**: 2509–2512.
- Macnab, R.M., & Ornston, K., (1977) Normal-to-Curly Flagella Transitions and their Role in Bacterial Tumbling. Stabilization of an Alternative Quaternary Structure by Mechanical Force. *Journal of Molecular Biology*. **112**: 1–30.
- Maddox, J.R., & Shapiro, L., (1993) Polar Location of the Chemoreceptor Complex in the *Escherichia coli* Cell. *Science*. **259**: 1717–1723.

- Magariyama, Y., Sugiyama, S., & Kudo, S., (2001) Bacterial Swimming Speed and Rotation Rate of Bundled Flagella. *FEMS microbiology letters*. **199**: 125–129.
- McNeill A., R., (2002) Principles of Animal Locomotion. *Princeton University Press*. p. 249-296.
- Maki, N., Gestwicki, J.E., Lake, E.M., Kiessling, L.L., & Adler, J., (2000) Motility and Chemotaxis of Filamentous Cells of *Escherichia coli*. *Journal of Bacteriology*. **182**: 4337–4342.
- Margolin, W., (2005) FtsZ and the Division of Prokaryotic Cells and Organelles. *Nature Reviews Molecular Cell Biology*. **6**: 862–871.
- Mesibov, R., & Adler, J., (1972) Chemotaxis Toward Amino Acids in *Escherichia coli*. *Journal of Bacteriology*. **112**: 315–326.
- Mitchell, J.G., (1991) The Influence of Cell Size on Marine Bacterial Motility and Energetics. *Microbial Ecology*. **22**: 227–238.
- Mitchell, J.G., (2002) The Energetics and Scaling of Search Strategies in Bacteria. *The American Naturalist*. **160**: 727–740.
- Mitchell, J.G., Pearson, L., Bonazinga, A., Dillon, S., Khouri, H., & Paxinos, R., (1995) Long Lag Times and High Velocities in the Motility of Natural Assemblages of Marine Bacteria. *Applied and Environmental Microbiology*. **61**: 877–882.

- Mitchell, J.G., & Kogure, K., (2006) Bacterial motility: Links to the Environment and a Driving Force for Microbial Physics: Bacterial Motility. *FEMS Microbiology Ecology*. **55**: 3–16.
- Molaei, M., Barry, M., Stocker, R., & Sheng, J., (2014) Failed Escape: Solid Surfaces Prevent Tumbling of Escherichia coli. *Physical Review Letters*. **113**: 068103.
- Nachtigall, W., (1981) Hydromechanics and Biology. *Biophysics of Structure and Mechanism*. **8**: 1–22.
- Purcell, E.M., (1977) Life at low Reynolds Number, *in: AIP Conference Proceedings*. p. 49.
- Reynolds, O., (1883) An Experimental Investigation of the Circumstances Which Determine Whether the Motion of Water Shall be Direct or Sinuous, and of the Law of Resistance in Parallel Channels. *Proceedings of the Royal Society of London*. **35**: 935–982.
- Rolinson, G.N., (1980) Effect of  $\beta$ -lactam Antibiotics on Bacterial Cell Growth Rate. *Journal of General Microbiology*. **120**: 317–323.
- Schuech, R., & Menden-Deuer, S., (2014) Going Ballistic in the Plankton: Anisotropic Swimming Behavior of Marine Protists. *Limnology & Oceanography: Fluids & Environments*. **4**: 1–16.
- Schulz, H.N., & Barker-Jorgensen, B., (2001) Big Bacteria. *Annual Reviews in Microbiology*. **55**: 105–137.

- Schwarz, U., & Leutgeb, W., (1971) Morphogenetic Aspects of Murein Structure and Biosynthesis. *Journal of bacteriology*. **106**: 588–595.
- Segall, J.E., Ishihara, A., & Berg, H.C., (1985) Chemotactic Signalling in Filamentous Cells of *Escherichia coli*. *Journal of bacteriology*. **161**: 51–59.
- Shih, Y.-L., Le, T., & Rothfield, L., (2003) Division Site Selection in *Escherichia coli* Involves Dynamic Redistribution of Min Proteins Within Coiled Structures that Extend Between the Two Cell Poles. *Proceedings of the National Academy of Sciences*. **100**: 7865–7870.
- Silverman, M., & Simon, M., (1974) Flagella Rotation and the Mechanism of Bacterial Motility. *Nature*. **249**: 73–74.
- Sleigh, M.A., (1991) Mechanisms of Flagellar Propulsion. *Protoplasma*. **164**: 45–53.
- Sommer, U., (1988) Some Size Relationships in Phytoflagellate Motility. *Hydrobiologia*. **161**: 125–131.
- Sourjik, V., (2004) Receptor Clustering and Signal Processing in *E. coli* Chemotaxis. *Trends in Microbiology*. **12**: 569–576.
- Spratt, B.G., (1975) Distinct Penicillin Binding Proteins Involved in the Division, Elongation, and Shape of *Escherichia coli* K12. *Proceedings of the National Academy of Sciences*. **72**: 2999–3003.

- Szmelcman, S., & Adler, J., (1976) Change in Membrane Potential During Bacterial Chemotaxis. *Proceedings of the National Academy of Sciences*. **73**: 4387–4391.
- Takeuchi, S., DiLuzio, W.R., Weibel, D.B., & Whitesides, G.M., (2005) Controlling the Shape of Filamentous Cells of *Escherichia coli*. *Nano letters*. **5**: 1819–1823.
- Taylor, G.I., (1922) Diffusion by Continuous Movements. *Proceedings of the London Mathematical Society*. **2**: 196– 212.
- Turner, L., Ryu, W.S., & Berg, H.C., (2000) Real-Time Imaging of Fluorescent Flagella Filaments. *Journal of Bacteriology*. **182**: 2793–2801.
- Van den Ent, F., & Lowe, J., (2001) Prokaryotic Origin of the Actin Cytoskeleton. *Nature*. **413**: 39–44.
- Visser, A.W., & Kiørboe, T., (2006) Plankton Motility Patterns and Encounter Rates. *Oecologia*. **148**: 538–546.
- Vogel, S., (1994) Life in Moving Fluids: The Physical Biology of Flow. *Princeton University Press*, Second Ed. p. 84-85.
- Vogel, S., (2008) Modes and Scaling in Aquatic Locomotion. *Integrative and Comparative Biology*. p. 1–11.
- Vogel, H.J., & Bonner, D.M., (1956) Acetylornithinase of *Escherichia coli*: Partial Purification and Some Properties. *Journal of Biological Chemistry*. **218**: 97–106.

- Wang, S., Arellano-Santoyo, H., Combs, P.A., & Shaevitz, J.W., (2010) Actin-like Cytoskeleton Filaments Contribute to Cell Mechanics in Bacteria. *Proceedings of the National Academy of Sciences*. **107**: 9182–9185.
- Weiss, D.S., (2004) Bacterial Cell Division and the Septal Ring: The Septal Ring. *Molecular Microbiology*. **54**: 588–597.
- Winet, H. (1973) Wall-drag on Free-moving Ciliated Microorganisms. *Journal of Experimental Biology*. **59**:753-766.
- Young, K.D., (2006) The Selective Value of Bacterial Shape. *Microbiology and Molecular Biology Reviews*. **70**(3): 660-703.
- Young, K.D., (2007) Bacterial Morphology: Why Have Different Shapes? *Current Opinion in Microbiology*. **10**: 596–600.

